

# Maximin Headway Control of Automated Vehicles for System Optimal Dynamic Traffic Assignment in General Networks

Jinxiao Du<sup>a</sup>, Wei Ma<sup>a,\*</sup>

<sup>a</sup>*Department of Civil and Environmental Engineering  
The Hong Kong Polytechnic University, Hong Kong SAR*

---

## Abstract

This study develops the headway control framework in a fully automated road network, as we believe headway of Automated Vehicles (AVs) is another influencing factor to traffic dynamics in addition to conventional vehicle behaviors (*e.g.* route and departure time choices). Specifically, we aim to search for the optimal time headway between AVs on each link that achieves the network-wide system optimal dynamic traffic assignment (SO-DTA). To this end, the headway-dependent fundamental diagram (HFD) and headway-dependent double queue model (HDQ) are developed to model the effect of dynamic headway on roads, and a dynamic network model is built. It is rigorously proved that the minimum headway could always achieve SO-DTA, yet the optimal headway is non-unique. Motivated by these two findings, this study defines a novel concept of maximin headway, which is the largest headway that still achieves SO-DTA in the network. Mathematical properties regarding maximin headway are analyzed and an efficient solution algorithm is developed. Numerical experiments on both a small and large network verify the effectiveness of the maximin headway control framework as well as the properties of maximin headway. This study sheds light on deriving the desired solution among the non-unique solutions in SO-DTA and provides implications regarding the safety margin of AVs under SO-DTA.

*Keywords:* Automated Vehicles (AVs), System Optimal Dynamic Traffic Assignment (SO-DTA), Headway Control, Maximin Optimization, Double Queue

---

## 1. Introduction

With the rapid development of advanced sensors, wireless communication, and artificial intelligence, it is envisioned that automated vehicles (AVs) will play a significant role in future intelligent transportation systems. Ultimately, the fully automated environment would be realized to significantly mitigate congestion and ensure safety in general urban networks (Wadud et al. 2016). Therefore, it is essential for public agencies (*e.g.*, Transport Department) and private sectors (*e.g.*, Transportation Network Companies) to understand the network-wide effects of AVs in the fully automated environment and to develop effective management and control schemes for AVs. However, recent studies mainly focus on the microscopic behaviors of AVs, while studies on the spatio-temporal effects of AVs in networked traffic dynamics are still lacking (Yu et al. 2021).

Among various traffic network models, system optimal dynamic traffic assignment (SO-DTA) quantifies the best possible performance of a traffic network given the dynamic network demand and supply. Both the optimal objective function (*i.e.*, the total travel time) and the optimal solution (*i.e.*, network dynamics under SO-DTA) could benchmark different traffic operation and management strategies and provide policy implications for decision-makers. Additionally, it is practical to control all the AVs to achieve SO-DTA under fully automated environments (Nguyen et al. 2021).

In this paper, we consider the headway control of AVs, in addition to the travelers' behaviors (*e.g.*, route and departure time choices). That is, AVs can decide the headway between each other according to the mobility and safety requirements of each road segment (Hatipoglu et al. 1996). In particular, headway refers to the time

---

\*Corresponding author

*Email addresses:* jinxiao.du@connect.polyu.hk (Jinxiao Du), wei.w.ma@polyu.edu.hk (Wei Ma)

headway throughout the paper. Existing studies have shown that different headway settings of AVs could affect the fundamental diagrams of each road (Zhou & Zhu 2020, Gong et al. 2016), hence affecting the solutions of SO-DTA. However, most current studies are at a microscopic level, while how the AV headway control could affect the network-wide SO-DTA is still an open question.

Intuitively, smaller AV headway yields higher road capacities and throughput, leading to shorter travel time, and hence SO-DTA can be achieved with the smallest AV headway. To verify this intuition, later this paper *analytically* proves that Observation 1 holds in general networks.

**Observation 1.** *Given a range of the AV headway, SO-DTA is always achieved when the AV headway is set as the smallest value in the range.*

Note that the range of AV headway depends on the minimum safety requirements of AVs, specifications of AVs, and the maximum capacity of the specific road (Li & Chen 2017). Furthermore, similar to the existing SO-DTA models (Shen & Zhang 2014), we have Observation 2 holds, indicating that SO-DTA may be achieved under different headway settings.

**Observation 2.** *There can be multiple AV headway settings yielding the same SO-DTA solution in general networks.*

Observation 2 inspires us to search for the second criterion in the SO-DTA problem. For AVs, safety is always an indispensable factor. For example, Li (2022) proved that there exists a trade-off between the time lag gap and the safety buffer that collectively constitutes the headway. Suppose the time lag gap is fixed because it is based on the vehicle specifications and mechanical properties, AVs could be safer when the headway becomes larger. Under the same traffic conditions, we expect to have larger headway between AVs.

In view of this, this paper proposes a novel concept of the maximin headway of AVs for SO-DTA, as defined in Definition 1.

**Definition 1** (Maximin Headway - Layman’s version). *The largest headway setting for AVs that still achieves the SO-DTA is referred to as the maximin headway of AVs.*

One can see that the maximin headway is the “largest” headway setting that achieves SO-DTA, meaning that such a headway setting is the “safest” under the SO-DTA. An illustration of the maximin headway is also presented in Figure 1. Existing literature mainly focuses on the solutions to SO-DTA (Zhang & Qian 2020, Qian et al. 2012), while this paper discusses the “best” solution among the non-unique solutions of SO-DTA for AVs, which we believe is interesting and unique. In particular, differences between minimum headway and maximin headway provide policy implications for road segment design and AV deployment.

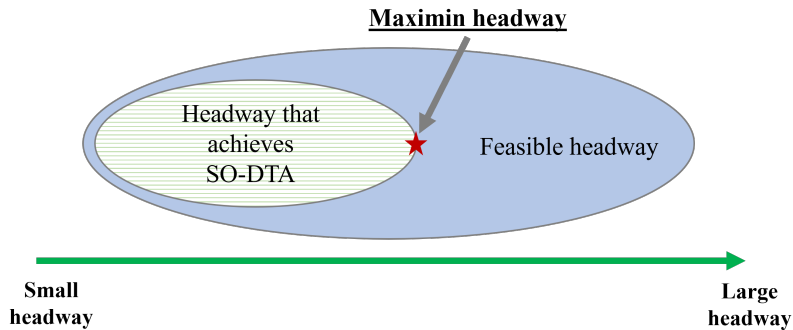


Figure 1: Illustration of the maximin headway for SO-DTA.

To summarize, this paper proposes a maximin headway control framework that achieves SO-DTA. Specifically, we first explore how the headway of AVs would affect the road fundamental diagram and develop a headway-dependent double queue model (HDQ), which is proved to be a generalized form of the double queue model (Ma et al. 2014). Then we formulate the network-wide traffic dynamics with SO-DTA for AVs, followed by the rigorous

proof that Observation 1 and Observation 2 hold. Then we formally define the maximin headway control for SO-DTA, propose a provable approach to solve it analytically, and show the uniqueness of the maximin headway. Lastly, numerical experiments are conducted on the small and large networks to verify our proofs.

The contributions of this paper are summarized as follows:

- The headway-dependent fundamental diagram (HFD) and double queue model (HDQ) are developed to depict the effects of AV headway on network-wide traffic dynamics.
- It is analytically proved that the SO-DTA can be achieved under minimum headway.
- We first time propose the maximin headway control of AVs for SO-DTA in general dynamic networks; the maximin headway is proved to be unique, and it can be obtained analytically using Linear Programming (LP).

The remainder of this paper is organized as follows: related literature is reviewed in Section 2. Section 3 presents headway-dependent flow dynamics using HFD and HDQ, Section 4 develops the formulation of optimal headway control, Section 5 proposes the formulation of maximin headway control and the corresponding solution algorithm, and Section 6 shows the numerical results in the small and large networks. Lastly, conclusions are drawn in section 7.

## 2. Literature review

In this section, we summarize the literature regarding the traffic network models for AVs. In particular, we compare with existing studies on dynamic link models, network models, and SO-DTA, to further highlight the contributions of this paper.

### 2.1. Dynamic link models

Dynamic link models are an essential component to model the flow dynamics on road segment, and it is necessary to develop an appropriate link model to depict the effects of AV headway control. The cell transmission model (CTM) is a classical link model and could capture congestion spillbacks (Daganzo 1995). However, CTM requires the decomposition of link into cells both in space and time, making the dimension of a DTA problem significantly increased. The link transmission model (LTM) is derived from the kinematic wave theory but does not require the decomposition of link (Yperman 2007). LTM considers the constraints on the sending flow and receiving flow, which are limited in the free-flow state and congested state respectively. Directly derived from LTM, Osorio et al. (2011) and Ma et al. (2014) propose the double queue model (DQ) to define the specific formulation of the downstream queue and upstream queue in a link for single-destination traffic networks. DQ is based on a forward free-flow travel time delay in downstream queue and a backward shockwave travel time delay in upstream queue. Besides, Ngoduy et al. (2021) proposes a multi-class two regime transmission model (MTTM) model to capture the evolution of the queue lengths, where a link is divided into two areas: free-flow area and congested area. Overall, none of the above mentioned models consider the effects of different AV headway on the road segment, and hence we call for a headway-dependent dynamic link model to depict the flow dynamics of AVs with different headway.

### 2.2. DTA with AVs

Dynamic traffic assignment (DTA) models are designed to explore the time-dependent traffic states pattern given a time-varying travel demand on general traffic networks (Szeto & Lo 2006). There are two representative types of DTA: dynamic user equilibrium (DUE) and system optimal dynamic traffic assignment (SO-DTA). SO-DTA quantifies the best possible performance of a traffic network based on the dynamic extension of Wardrop's second principle (Wardrop 1952). For its advantage of exploring the spatial-temporal traffic dynamics to achieve the best performance of traffic networks, the research of the application of SO-DTA problem focuses on many different areas, such as emission reduction (Lu et al. 2016, Ma et al. 2017, Long et al. 2018, Tan et al. 2021), congestion mitigation (Levin 2017, Samaranayake et al. 2018, Liu et al. 2020), parking services (Levin 2019, Qian & Rajagopal 2014), traffic signal control (Lo 2001, Han et al. 2016), emergency evacuation (Liu et al. 2006, Chiu et al. 2007) and network design (Waller & Ziliaskopoulos 2001, Waller et al. 2006).

Different from human-driven vehicles (HVs), AVs show great potential in improving control efficiency and may play an important role in achieving SO-DTA (Wang et al. 2018). The current research on traffic assignment with AVs is summarized in Table 1. For the static traffic assignment problem of AVs, Chen et al. (2016) proposes a mathematical model to derive an optimal AV lane control with mixed traffic, where AV lanes are only permitted for AVs and it is necessary to specify the deployment plan. Bagloee et al. (2017) focuses on a static traffic assignment problem on a mixed traffic where AVs are seeking for system optimal (SO) and HVs are seeking for user equilibrium (UE), and considers the influence of many realistic features in the solution, such as road capacity and elastic demand. Chen et al. (2017) presents an optimal AVs zones design framework to improve the performance of the whole traffic network, where the government may make a plan of AVs zones only allowing AVs to enter to promote the adoption of AVs in the future. Zhang & Nie (2018) proposes a route control scheme to balance the system efficiency and the control intensity by controlling a relatively small portion of all vehicles. Wang et al. (2019) addresses the multi-class traffic assignment problem by assuming AVs follow SO and HVs follow cross-nested logit (CNL) stochastic user equilibrium (SUE) to capture HV drivers’ uncertainty due to their limited knowledge of traffic conditions in the whole network. Wang et al. (2020) develops a mixed behavioral equilibrium model in a mixed traffic considering different mode choices for HVs and AVs.

Reference	Type	HV	AV	Description
Levin & Boyles (2016)	Dynamic	DUE	DUE	A multi-class CTM model for mixed traffic
Chen et al. (2016)	Static	UE	UE	An optimal AV lanes control framework for mixed traffic
Bagloee et al. (2017)	Static	UE	SO	The mixed traffic network with elastic demand
Chen et al. (2017)	Static	UE	SO	Optimal design of AV zones for mixed traffic
Zhang & Nie (2018)	Static	UE	SO	A route control scheme to balance efficiency and control
Wang et al. (2019)	Static	CNL	UE	A multi-class traffic assignment model for mixed traffic
Wang et al. (2020)	Static	SUE	SO	A mixed equilibrium model with mode choice
Ngoduy et al. (2021)	Dynamic	SO-DTA	SO-DTA	Impact of AVs in traffic network by multi-class SO-DTA
Seo & Asakura (2022)	Dynamic	\	SO-DTA	A unified optimization strategy framework for shared AVs
<b>This paper</b>	Dynamic	\	SO-DTA	Maximin AV headway control for SO-DTA on general networks

Table 1: Literature summary of traffic assignment with AVs.

In summary, the work related to the traffic assignment problem of AVs is mainly static and there is few work exploring how AV headway control would affect the traffic states in whole general networks as a SO-DTA problem. There is few work discussing the roles of headway in the control of AVs. Therefore, this paper is designed to propose an optimal AV headway control framework for SO-DTA in general networks.

### 2.3. Uniqueness of SO-DTA

The solution of SO-DTA provides valuable insights for decision-makers to develop traffic management strategies (van Essen et al. 2016). Most of the related works focus on the solution algorithm of SO-DTA (Chow 2009, Zhang & Qian 2020, Qian et al. 2012, Long & Szeto 2019), and there is a few work discussing the non-uniqueness and properties of the solutions of SO-DTA. For example, Shen & Zhang (2014) proves that SO-DTA may have multiple solutions with same objective but different queue locations in networks. To explore the optimal queue distribution for the solution of SO-DTA, Ma et al. (2014) proposes the solution algorithm and discusses the existence of the free-flow optimal solution of SO-DTA that all vehicles are only allowed to wait in the origin nodes, and Ngoduy et al. (2016) optimizes the heterogeneity of the queue lengths and the total queue lengths in traffic networks for all solutions of SO-DTA. Though both of above work discuss the non-uniqueness of the solutions of SO-DTA and propose the criteria to “pick up” the desired solution of SO-DTA, the criteria of both works are mainly related to congestion patterns. In reality, decision-makers could develop traffic management strategies considering different perspectives. Therefore, this paper discusses the “safest” solution among the non-unique solutions of SO-DTA and proposes the maximin headway in this problem as the largest headway solution in SO-DTA.

## 3. Modeling headway-dependent flow dynamics

In this section, we first propose the headway-dependent fundamental diagram (HFD) and develop the headway-dependent double queue (HDQ) model, which is proved to be a generalized form of DQ, and then the network-wide

flow dynamics are modeled through a series of linear constraints.

### 3.1. Notations

The road network is represented as a directed graph  $G(V,E)$ , where  $V$  is the set of all nodes including dummy nodes and  $E$  is the set of all links including O-D connectors. We denote  $\widetilde{R}$  as the set of dummy origins and  $\widetilde{S}$  as the set of dummy destinations. Naturally, we have  $\widetilde{R} \subset V$  and  $\widetilde{S} \subset V$ . The frequently used notations are stated in Table A.4 in Appendix A.

### 3.2. Headway-Dependent Fundamental Diagram

This section explores how different headway would affect the fundamental diagram. Without loss of generality, it is assumed that the headway and length of AV are homogeneous. Then we present the fundamental diagram for AVs based on the results by Zhou & Zhu (2020). Considering link  $(i, j)$ , we denote  $\Delta_{x_{i,j}}$  as the spacing of AVs in link  $(i, j)$ ,  $v_{i,j}$  as the speed of AVs on link  $(i, j)$ ,  $h_{i,j}$  as the headway of AVs in link  $(i, j)$  and  $L$  as the length of each AV. The relationship between the headway  $h_{i,j}$  and spacing  $\Delta_{x_{i,j}}$  can be described as follows:

$$\Delta_{x_{i,j}} = h_{i,j}v_{i,j} + L.$$

Besides, the relationship between the spacing  $\Delta_{x_{i,j}}$  and density  $\rho_{i,j}$  is shown as follows:

$$\Delta_{x_{i,j}} = \frac{1}{\rho_{i,j}}.$$

The speed  $v_{i,j}$  should be limited within free-flow speed  $v_{i,j}^f$  as follows:

$$0 \leq v_{i,j} \leq v_{i,j}^f.$$

Combining the above equations, we have Equation 1 to represent the fundamental diagram of AVs denoted as  $f_{i,j}^{FD}(t)$  for  $(i, j) \in E \setminus (L_R \cup L_S)$  and  $t \in [0, T]$ , where  $L_R$  and  $L_S$  represent the set of origin and destination connectors, respectively.

$$f_{i,j}^{FD}(t) = \begin{cases} v_{i,j}^f \rho_{i,j}(t), & 0 \leq \rho_{i,j}(t) < \frac{1}{h_{i,j}(t)v_{i,j}^f + L} \\ \frac{1 - \rho_{i,j}(t)L}{h_{i,j}(t)}, & \frac{1}{h_{i,j}(t)v_{i,j}^f + L} \leq \rho_{i,j}(t) \leq \frac{1}{L} \end{cases} \quad (1)$$

where  $\rho_{i,j}(t)$  and  $h_{i,j}(t)$  are the density of the flow area and headway of link  $(i, j)$  at time  $t$ , respectively. Figure 2 shows the fundamental diagram of AVs with different headway based on Equation 1. This figure is also validated by the experimental results from Shi & Li (2021), which empirically validates the fundamental diagram by collecting GPS trajectories of a platoon of AVs.

As shown in Figure 2, headway could affect the fundamental diagram of AVs in the following aspects:

- Scope of free-flow region: a smaller headway corresponds to a larger scope of free-flow region.
- Upper bound of flow: a smaller headway corresponds to a larger upper bound of flow.
- Shockwave travel speed: a smaller headway corresponds to a higher shockwave travel speed.

Besides, we suppose the first AV entering an empty link would drive at a free-flow travel speed for link  $(i, j) \in E \setminus (L_R \cup L_S)$  and  $t \in [0, T]$ . Then the headway-dependent fundamental diagram (HFD) is presented in Equation 2:

$$f_{i,j}(t) = \begin{cases} 0, & \text{if } \rho_{i,j}(t - \frac{L_{i,j}}{v_{i,j}^f}) = 0 \\ f_{i,j}^{FD}(t), & \text{otherwise} \end{cases} \quad (2)$$

where  $f_{i,j}(t)$  is the inflow at the boundary of the flow area and buffer area of link  $(i, j)$  at time  $t$ . The conservation law of traffic flow is shown as follows:

$$\rho_t + f_x = 0.$$

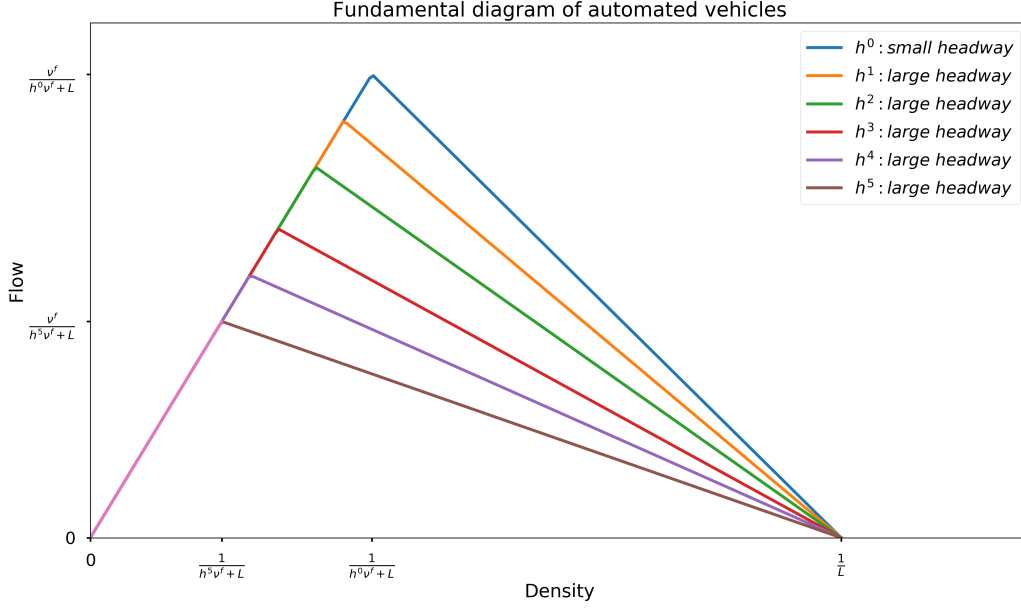


Figure 2: Fundamental diagram of AVs with different headway.

Assuming the density is homogeneous in a link, the change rate of density is presented in Equation 3 for  $(i, j) \in E \setminus (L_R \cup L_S)$ ,  $s' \in \tilde{S}$  and  $t \in [0, T]$ :

$$\dot{\rho}_{i,j}^{s'}(t) = \frac{u_{i,j}^{s'}(t) - f_{i,j}^{s'}(t)}{L_{i,j}}, \quad (3)$$

where  $\rho_{i,j}^{s'}(t)$ ,  $u_{i,j}^{s'}(t)$  and  $f_{i,j}^{s'}(t)$  are the density of the flow area, inflow of the flow area and inflow at the boundary of the flow area and buffer area with destination  $s'$  of link  $(i, j)$  at time  $t$ ;  $L_{i,j}$  is the length of link  $(i, j)$ . Therefore, the dynamic link density  $\rho_{i,j}(t)$  for  $(i, j) \in E \setminus (L_R \cup L_S)$ ,  $s' \in \tilde{S}$  and  $t \in [0, T]$  is represented as follows:

$$\dot{\rho}_{i,j}(t) = \frac{u_{i,j}(t) - f_{i,j}(t)}{L_{i,j}}, \quad (4)$$

where  $u_{i,j}(t)$  is the inflow of the flow area of link  $(i, j)$  at time  $t$ .

Besides,  $\tau_{i,j}^w(t)$  represents the shockwave travel time on link  $(i, j)$  at time  $t$ . If the fundamental diagram is fixed, we have a constant shockwave travel time  $\tau_{i,j}^w = \frac{L_{i,j}}{v_{i,j}^w}$ , where  $v_{i,j}^w$  is the shockwave speed on link  $(i, j)$ . However, in HFD, the shockwave speed is also dynamic given different headway. Equation 5 indicates that the shockwave travel time should satisfy Equation 5 for  $(i, j) \in E \setminus (L_R \cup L_S)$ ,  $s' \in \tilde{S}$  and  $t \in [0, T]$ .

$$\int_{t-\tau_{i,j}^w(t)}^t \frac{L}{h_{i,j}(t)} dt = L_{i,j} \quad (5)$$

### 3.3. Headway-dependent double queue model

This section proposes a dynamic link model considering time-dependent AV headway, namely the headway-dependent double queue (HDQ) model. We further prove HDQ is a generalized form of the double queue (DQ) model.

In HDQ, each link is divided into two areas: flow area and buffer area. The flow area depicts the traffic flow dynamics behavior and captures the upstream queue in the link, and we suppose the traffic flow would propagate

based on HFD. The buffer area captures the downstream queue in the link and the maximum number of queued vehicle is limited based on the holding capacity in the buffer area (Guo & Ban 2020). An illustration of the HDQ is shown in Figure 3. One can see that the HDQ is inspired by the MTTM and DQ model, and it shares similarities with the Spatial Queue model (Gawron 1998).

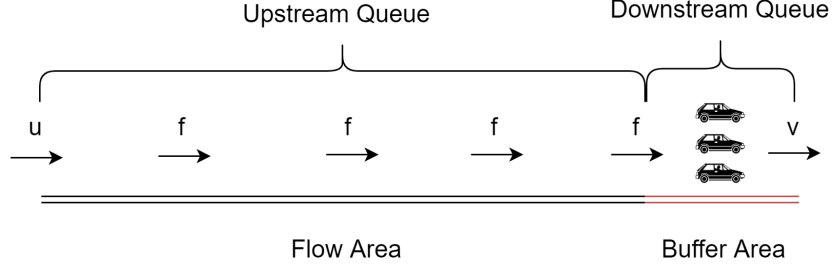


Figure 3: Flow area and buffer area in a link.

The HDQ has following characteristics that are different from the DQ and MTTM:

- The MTTM overlooks the possible congestion in the flow area, while the HDQ consider both upstream and downstream queues.
- Comparing to the DQ, the HDQ makes use of the variable  $f$  to represent the effect of headway control on the traffic states and network conditions.

The cumulative flow for  $(i, j) \in E$  and  $t \in [0, T]$  is defined as follows:

$$U_{i,j}(t) = \int_0^t u_{i,j}(t) dt, \quad V_{i,j}(t) = \int_0^t v_{i,j}(t) dt, \quad F_{i,j}(t) = \int_0^t f_{i,j}(t) dt,$$

where  $U_{i,j}(t)$ ,  $V_{i,j}(t)$  and  $F_{i,j}(t)$  are the cumulative inflow of the flow area, cumulative outflow of the buffer area and cumulative inflow at the boundary of the flow area and buffer area of link  $(i, j)$  at time  $t$ , respectively.

Then the downstream queue and upstream queue in HDQ for  $(i, j) \in E$  and  $t \in [0, T]$  are presented as follows:

$$q_{i,j}^{\mathcal{D}}(t) = \int_0^t f_{i,j}(t) dt - \int_0^t v_{i,j}(t) dt + q_{i,j}^{\mathcal{D}}(0) = F_{i,j}(t) - V_{i,j}(t), \quad (6)$$

$$q_{i,j}^{\mathcal{U}}(t) = \int_0^t u_{i,j}(t) dt - \int_0^{t-\tau_{i,j}^w} f_{i,j}(t) dt + q_{i,j}^{\mathcal{U}}(0) = U_{i,j}(t) - F_{i,j}(t - \tau_{i,j}^w(t)), \quad (7)$$

where  $q_{i,j}^{\mathcal{D}}(t)$  and  $q_{i,j}^{\mathcal{U}}(t)$  represent the downstream and upstream queue of link  $(i, j)$  at time  $t$  in HDQ, respectively.

Proposition 1 presents the relationship between the DQ and HDQ, indicating that HDQ could be reduced to DQ under its assumption.

**Proposition 1** (Reduction of HDQ to DQ). *HDQ is a generalized form of DQ by incorporating the influence of headway; HDQ could be reduced to the DQ under the assumption of DQ.*

*Proof.* See Appendix B. □

To consider general networks with multiple destinations, we further represent the downstream and upstream queue in HDQ by Equations 8 and 9 for  $(i, j) \in E$ ,  $s' \in \tilde{S}$  and  $t \in [0, T]$ .

$$q_{i,j}^{\mathcal{D},s'}(t) = \int_0^t f_{i,j}^{s'}(t) dt - \int_0^t v_{i,j}^{s'}(t) dt + q_{i,j}^{\mathcal{D},s'}(0), \quad (8)$$

$$q_{i,j}^{\mathcal{U},s'}(t) = \int_0^t u_{i,j}^{s'}(t) dt - \int_0^{t-\tau_{i,j}^w(t)} f_{i,j}^{s'}(t) dt + q_{i,j}^{\mathcal{U},s'}(0), \quad (9)$$

where  $q_{i,j}^{\mathcal{D},s'}(t)$ ,  $q_{i,j}^{\mathcal{U},s'}(t)$  and  $v_{i,j}^{s'}(t)$  are the downstream queue, upstream queue and outflow of the buffer area with destination  $s'$  of link  $(i, j)$  at time  $t$ , respectively.

We further have Equations 10 and 11 hold, meaning that traffic flow dynamics variables are the summation of their destination-specified variables for  $(i, j) \in E$ ,  $s' \in \bar{S}$  and  $t \in [0, T]$ .

$$q_{i,j}^{\mathcal{D}}(t) = \sum_{s'} q_{i,j}^{\mathcal{D},s'}(t); \quad q_{i,j}^{\mathcal{U}}(t) = \sum_{s'} q_{i,j}^{\mathcal{U},s'}(t); \quad \rho_{i,j}(t) = \sum_{s'} \rho_{i,j}^{s'}(t). \quad (10)$$

$$u_{i,j}(t) = \sum_{s'} u_{i,j}^{s'}(t); \quad f_{i,j}(t) = \sum_{s'} f_{i,j}^{s'}(t); \quad v_{i,j}(t) = \sum_{s'} v_{i,j}^{s'}(t). \quad (11)$$

Additionally, Equation 12 and 13 indicate that the downstream queue, upstream queue, inflow rate and outflow rate are bounded by their respective capacity for  $(i, j) \in E \setminus (L_R \cup L_S)$ ,  $s' \in \bar{S}$  and  $t \in [0, T]$ .

$$q_{i,j}^{\mathcal{D}}(t) \leq \bar{Q}_{i,j}^{\mathcal{D}}, \quad q_{i,j}^{\mathcal{U}}(t) \leq \bar{Q}_{i,j}^{\mathcal{U}}, \quad (12)$$

$$u_{i,j}(t) \leq \bar{C}_{i,j}^{\mu}, \quad v_{i,j}(t) \leq \bar{C}_{i,j}^{\nu}, \quad (13)$$

where  $\bar{Q}_{i,j}^{\mathcal{D}}$  and  $\bar{Q}_{i,j}^{\mathcal{U}}$  are the downstream queue capacity and upstream queue capacity, respectively;  $\bar{C}_{i,j}^{\mu}$  and  $\bar{C}_{i,j}^{\nu}$  are the inflow and outflow capacity of link  $(i, j)$  at time  $t$ , respectively. We further have Proposition 2 indicating that the impact to the maximal flow rate of the link is dependent on the HDQ.

**Proposition 2** (Headway-dependent flow rate bounds). *The upper bounds of the inflow rate  $u_{i,j}(t)$  and outflow rate  $v_{i,j}(t)$  are dependent on the upstream queue  $q_{i,j}^{\mathcal{U}}(t)$  and downstream queue  $q_{i,j}^{\mathcal{D}}(t)$ , respectively, and their relation is shown as follows.*

$$u_{i,j}(t) \leq \begin{cases} \bar{C}_{i,j}^{\mu}, & q_{i,j}^{\mathcal{U}}(t) < \bar{Q}_{i,j}^{\mathcal{U}} \\ \min\{f_{i,j}(t - \tau_{i,j}^w(t)), \bar{C}_{i,j}^{\mu}\}, & q_{i,j}^{\mathcal{U}}(t) = \bar{Q}_{i,j}^{\mathcal{U}} \end{cases}$$

$$v_{i,j}(t) \leq \begin{cases} \bar{C}_{i,j}^{\nu}, & q_{i,j}^{\mathcal{D}}(t) > 0 \\ \min\{f_{i,j}(t), \bar{C}_{i,j}^{\nu}\}, & q_{i,j}^{\mathcal{D}}(t) = 0 \end{cases}$$

*Proof.* See Appendix C. □

### 3.4. Dynamic network traffic model

This section models the network-wide effects of AV headway control by developing a dynamic network model. The flow conservation at nodes is stated in Equation 14 for  $i \in N \setminus (\bar{R} \cup \bar{S})$ ,  $s' \in \bar{S}$  and  $t \in [0, T]$ .

$$\sum_p v_{p,i}^{s'}(t) = \sum_j u_{i,j}^{s'}(t) \quad (14)$$

The link conservation is ensured through the HDQ model. Equation 15 presents the non-negative constraint of all the variables involved for  $(i, j) \in E$ ,  $s' \in \bar{S}$  and  $t \in [0, T]$ .

$$\rho_{i,j}^{s'}(t), u_{i,j}^{s'}(t), f_{i,j}^{s'}(t), v_{i,j}^{s'}(t), q_{i,j}^{\mathcal{D},s'}(t), q_{i,j}^{\mathcal{U},s'}(t) \geq 0 \quad (15)$$

Besides, the number of AVs in link  $(i, j)$  with destination  $s'$  at time  $t$  could be represented as the sum of number of AVs in the flow area and buffer area, as shown in Equation 16.

$$\begin{aligned} N_{i,j}^{s'}(t) &= \int_0^t u_{i,j}^{s'}(t) dt - \int_0^t v_{i,j}^{s'}(t) dt \\ &= \int_0^t u_{i,j}^{s'}(t) dt - \int_0^t f_{i,j}^{s'}(t) dt + \int_0^t f_{i,j}^{s'}(t) dt - \int_0^t v_{i,j}^{s'}(t) dt \\ &= L_{i,j} \rho_{i,j}^{s'}(t) + q_{i,j}^{\mathcal{D},s'}(t) \end{aligned} \quad (16)$$

The initial condition of the network is stated in Equation 17 for  $(i, j) \in E$ ,  $s' \in \bar{S}$  and  $t \in [0, T]$ , which guarantees the whole traffic network is empty before loading.



$$\rho_{i,j}(0), q_{i,j}^{\mathcal{D},s'}(0) = 0 \quad (17)$$

The end condition constraint is presented in Equation 18 for  $(i, j) \in E$ ,  $s' \in \tilde{S}$  and  $t \in [0, T]$ , which guarantees the whole traffic network is empty in the end.

$$q_{i,j}^{\mathcal{D},s'}(T) = 0, \rho_{i,j}(T) < \frac{1}{L_{i,j}} \quad (18)$$

Importantly, for the change rate of link density can be represented by  $\dot{\rho}_{i,j}(t) = -\frac{v_{i,j}^f \rho_{i,j}(t)}{L_{i,j}}$ ,  $t \geq t_0$  based on Equation 4 when  $u_{i,j}(t) = 0$ . This represents the scenario in which no vehicles will enter the link when  $\rho_{i,j}(t_0) > 0$ .  $\rho_{i,j}(t)$  has the shape of the negative exponential function, and hence it will take infinite time to make  $\rho_{i,j}(t) = 0$ . In order to avoid this situation, we set the end constraint of the flow area in link  $(i, j)$  as  $\rho_{i,j}(T) < \frac{1}{L_{i,j}}$ , which means that we suppose the flow area is empty when the number of vehicles in flow area is smaller than 1 at the end time  $T$ . Furthermore, we could also set a large positive constant  $c$  as  $\rho_{i,j}(T) < \frac{1}{cL_{i,j}}$  to ensure the vehicles in total network is close to 0 at end time  $T$ .

Equation 19 depicts the travel demand entering the origin connectors for  $r \in \tilde{R}$ ,  $s' \in \tilde{S}$  and  $t \in [0, T]$ :

$$f_{r',r}^{s'}(t) = \begin{cases} d_{r',s'}(t), & 0 \leq t \leq T_1 \\ 0, & T_1 < t \leq T \end{cases} \quad (19)$$

where  $d_{r',s'}(t)$  represents the travel demand of O-D pair  $(r', s')$  at time  $t$ .

Additionally, Equation 20 limits the minimum and maximum headway for  $(i, j) \in E \setminus (L_R \cup L_S)$ ,  $s' \in \tilde{S}$  and  $t \in [0, T]$ .

$$h_{i,j}^{\min} \leq h_{i,j}(t) \leq h_{i,j}^{\max} \quad (20)$$

#### 4. Optimal headway control

In this section, we first formulate the continuous and discretized headway control for SO-DTA. Then we prove that the minimum headway control could achieve SO-DTA, and it is not the unique solution.

##### 4.1. Continuous-time formulation

The objective of the SO-DTA aims to minimize total travel time (TTT), which equals to the sum of the travel time on road networks and the waiting time at origins, as represented by Equation 21. The decision variables include traffic dynamics  $\mathbf{x}$  and headway  $\mathbf{h}$ .

$$\min_{\mathbf{x}, \mathbf{h}} TTT = \int_0^T \left( \sum_{r'} \int_0^t v_{r',r}(t) dt - \sum_{s'} \int_0^t u_{s,s'}(t) dt \right) dt + \int_0^T \sum_{(r',s')} q_{r',r}^{\mathcal{D},s'}(t) dt \quad (21)$$

subject to:

- Headway-dependent fundamental diagram constraints: Eqs. (1)-(5)
- Headway-dependent double queue constraints: Eqs. (8)-(13)
- Flow conservation constraints: Eq. (14)
- Non-negative constraints: Eq. (15)
- Initial constraints: Eq. (17)
- End constraints: Eq. (18)
- Other constraints: Eqs. (19)-(20)

Proposition 3 presents the feasibility of the proposed optimal headway control problem, where  $T_l$ ,  $n^{r',s'}$ ,  $P^{r',s'}$ ,  $T_{i,j}^{r',s'}$  and  $\delta_{i,j}^{P^{r',s'}}$  are defined in Appendix D.

**Proposition 3** (Feasibility). *If  $T > T_l + \sum_{(r',s')} n^{r',s'} \sum_{(i,j)} T_{i,j}^{r',s'} \delta_{i,j}^{P^{r',s'}}$ , the optimal headway control problem in Equation 21 is always feasible.*

*Proof sketch.* It is obvious that if we choose a large enough time horizon  $T$ , the problem is always feasible, which means all AVs would arrive at their destinations before  $T$ . So the basic idea for the proof is to find a large enough  $T$  and construct a feasible solution under  $T$ . Details are presented in Appendix D.  $\square$

#### 4.2. Discretized-time formulation

This section discretizes the formulation proposed in Section 4.1. We set  $T = N\Delta_t$ , where  $N$  represents the number of time intervals and  $\Delta_t$  represents the length of a time interval. We choose a small  $\Delta_t$  such that  $\Delta_t L < \min\{L_{i,j} h_{i,j}^{min}\}$  to have a non-zero shockwave travel time. The continuous formulation is non-linear programming due to the headway-dependent fundamental diagram constraints.

To identify the congestion and non-congestion region in HFD by Equation 1, we introduce the binary variables  $\delta_{i,j}(k)$  to indicate whether the flow area of link  $(i, j)$  in the  $k$ th time interval is congested or not. Hence constraint 2 could be equivalently converted to a binary constraint. Other variables are also discretized and a summary of the notations is shown in Table 2.

Notation	Description
$\rho_{i,j}(k)$	Density of the flow area of link $(i, j)$ in the $k$ th time interval
$\rho_{i,j}^{s'}(k)$	Density of the flow area of link $(i, j)$ with destination $s'$ in the $k$ th time interval
$q_{i,j}^D(k)$	Downstream queue of link $(i, j)$ in the $k$ th time interval
$q_{i,j}^{D,s'}(k)$	Downstream queue of link $(i, j)$ with destination $s'$ in the $k$ th time interval
$q_{i,j}^U(k)$	Upstream queue of link $(i, j)$ in the $k$ th time interval
$q_{i,j}^{U,s'}(k)$	Upstream queue of link $(i, j)$ with destination $s'$ in the $k$ th time interval
$u_{i,j}(k)$	Inflow of the flow area of link $(i, j)$ in the $k$ th time interval
$u_{i,j}^{s'}(k)$	Inflow of the flow area of link $(i, j)$ with destination $s'$ in the $k$ th time interval
$f_{i,j}(k)$	Inflow at the boundary of the flow area and buffer area of link $(i, j)$ in the $k$ th time interval
$f_{i,j}^{s'}(k)$	Inflow at the boundary of the flow area and buffer area of link $(i, j)$ with destination $s'$ in the $k$ th time interval
$v_{i,j}(k)$	Outflow of the buffer area of link $(i, j)$ in the $k$ th time interval
$v_{i,j}^{s'}(k)$	Outflow of the buffer area of link $(i, j)$ with destination $s'$ in the $k$ th time interval
$h_{i,j}(k)$	Headway of automated vehicles in link $(i, j)$ and $k$ th time interval
$\delta_{i,j}(k)$	Binary variable to indicate whether congested in the flow area of link $(i, j)$ in the $k$ th time interval
$n_{i,j}^w(k)$	Shockwave travel time on link $(i, j)$ in the $k$ th time interval

Table 2: Notations in the discretized formulation.

We are now ready to present the discretized version of the headway-dependent SO-DTA formulation as follows:

$$\min_{\mathbf{x}, \mathbf{h}} TTT = \sum_{r'} \sum_{k=1}^N \Delta_t \left( \sum_{l=1}^k \Delta_t v_{r',r}(l) \right) - \sum_{s'} \sum_{k=1}^N \Delta_t \left( \sum_{l=1}^k \Delta_t u_{s,s'}(l) \right) + \sum_{(r',s')} \sum_{k=1}^N \Delta_t q_{r',r}^{D,s'}(k) \quad (22)$$

subject to

1. Headway-dependent fundamental diagram constraints for  $(i, j) \in E \setminus (L_R \cup L_S)$ ,  $s' \in \tilde{S}$  and  $1 \leq k \leq N$ . We relax the assumption of Equation 2 as  $f_{i,j}(k) = f_{i,j}^{FD}(k)$ .

$$\text{if } \delta_{i,j}(k) = 0 :$$

$$0 \leq \rho_{i,j}(k) < \frac{1}{h_{i,j}(k) v_{i,j}^f + L} \quad (23)$$

$$f_{i,j}(k) = v_{i,j}^f \rho_{i,j}(k)$$

if  $\delta_{i,j}(k) = 1$  :

$$\frac{1}{h_{i,j}(k)v_{i,j}^f + L} \leq \rho_{i,j}(k) \leq \frac{1}{L} \quad (24)$$

$$f_{i,j}(k) = \frac{1 - \rho_{i,j}(k)L}{h_{i,j}(k)}$$

$$\rho_{i,j}^{s'}(k) = \rho_{i,j}^{s'}(k-1) + \Delta_t \frac{u_{i,j}^{s'}(k) - f_{i,j}^{s'}(k)}{L_{i,j}} \quad (25)$$

The discretized form of Equation 5 representing the shockwave travel time is shown as follows.

$$\sum_{l=k-n_{i,j}^w(k)}^k \Delta_t \frac{L}{h_{i,j}(l)} \leq L_{i,j}$$

$$\sum_{l=k-n_{i,j}^w(k)-1}^k \Delta_t \frac{L}{h_{i,j}(l)} > L_{i,j}$$

We assume that shockwave travel time  $n_{i,j}^w(k)$  is only determined by the headway  $h_{i,j}(k)$  in Equation 26 and 27.

$$n_{i,j}^w(k) \Delta_t \frac{L}{h_{i,j}(k)} \leq L_{i,j} \quad (26)$$

$$(n_{i,j}^w(k) + 1) \Delta_t \frac{L}{h_{i,j}(k)} > L_{i,j} \quad (27)$$

2. Headway-dependent double queue constraints constraints for  $s' \in \tilde{S}$  and  $1 \leq k \leq N$ . We limit  $(i, j) \in E$  in Equations 28 to 31 and  $(i, j) \in E \setminus (L_R \cup L_S)$  in Equations 32 to 33.

$$q_{i,j}^{\mathcal{D},s'}(k) = \sum_{l=0}^k \Delta_t f_{i,j}^{s'}(l) - \sum_{l=0}^k \Delta_t v_{i,j}^{s'}(l) + q_{i,j}^{\mathcal{D},s'}(0) \quad (28)$$

$$q_{i,j}^{\mathcal{U},s'}(k) = \sum_{l=0}^k \Delta_t u_{i,j}^{s'}(l) - \sum_{l=0}^{k-n_{i,j}^w(k)} \Delta_t f_{i,j}^{s'}(l) + q_{i,j}^{\mathcal{U},s'}(0) \quad (29)$$

$$q_{i,j}^{\mathcal{D}}(k) = \sum_{s'} q_{i,j}^{\mathcal{D},s'}(k); \quad q_{i,j}^{\mathcal{U}}(k) = \sum_{s'} q_{i,j}^{\mathcal{U},s'}(k); \quad \rho_{i,j}(k) = \sum_{s'} \rho_{i,j}^{s'}(k) \quad (30)$$

$$u_{i,j}(k) = \sum_{s'} u_{i,j}^{s'}(k); \quad f_{i,j}(k) = \sum_{s'} f_{i,j}^{s'}(k); \quad v_{i,j}(k) = \sum_{s'} v_{i,j}^{s'}(k) \quad (31)$$

$$q_{i,j}^{\mathcal{D}}(k) \leq \bar{Q}_{i,j}^{\mathcal{D}}; \quad q_{i,j}^{\mathcal{U}}(k) \leq \bar{Q}_{i,j}^{\mathcal{U}} \quad (32)$$

$$u_{i,j}(k) \leq \bar{C}_{i,j}^{\mathcal{U}}; \quad v_{i,j}(k) \leq \bar{C}_{i,j}^{\mathcal{V}} \quad (33)$$

3. Flow conservation constraints for  $i \in N \setminus (\tilde{R} \cup \tilde{S})$ ,  $s' \in \tilde{S}$  and  $1 \leq k \leq N$ .

$$\sum_p v_{p,i}^{s'}(k) = \sum_j u_{i,j}^{s'}(k) \quad (34)$$

4. Non-negative Constraint for  $(i, j) \in E$ ,  $s' \in \tilde{S}$  and  $1 \leq k \leq N$ .

$$\rho_{i,j}^{s'}(k), u_{i,j}^{s'}(k), f_{i,j}^{s'}(k), v_{i,j}^{s'}(k), q_{i,j}^{\mathcal{D},s'}(k), q_{i,j}^{\mathcal{U},s'}(k) \geq 0 \quad (35)$$

4. Initial condition constraint for  $(i, j) \in E$  and  $s' \in \widetilde{S}$ .

$$\rho_{i,j}(0), q_{i,j}^{\mathcal{D},s'}(0) = 0 \quad (36)$$

5. End condition constraint for  $(i, j) \in E$  and  $s' \in \widetilde{S}$ .

$$q_{i,j}^{\mathcal{D},s'}(N) = 0, \rho_{i,j}(N) < \frac{1}{L_{i,j}} \quad (37)$$

6. Other constraints for  $(i, j) \in E \setminus (L_R \cup L_S)$ ,  $r' \in \widetilde{R}$ ,  $s' \in \widetilde{S}$  and  $1 \leq k \leq N$ , where  $d_{r',s'}(k)$  represents the travel demand of O-D pair  $(r', s')$  in the  $k$ th time interval and  $n_1 = \frac{T_1}{\Delta_t}$ .

$$f_{r',s'}^{s'}(k) = \begin{cases} d_{r',s'}(k), & 1 \leq k \leq n_1 \\ 0, & n_1 < k \leq N \end{cases} \quad (38)$$

$$h_{i,j}^{\min} \leq h_{i,j}(k) \leq h_{i,j}^{\max} \quad (39)$$

We define the minimum total travel time and optimal headway of the discretized form of SO-DTA for Equations 22 to 39 in Definition 2.

**Definition 2.**  $\forall \mathbf{h}$  satisfies  $h_{i,j}^{\min} \leq h_{i,j}(k) \leq h_{i,j}^{\max}$  for each element, if  $\exists \mathbf{x}$  satisfies Equations 23 to 38, then  $\mathbf{h}$  and  $\mathbf{x}$  constitute a feasible solution of SO-DTA problem, denote the total travel time as  $TTT(\mathbf{x})$  and the set of feasible traffic dynamics under  $\mathbf{h}$  as  $\Omega_{\mathbf{h}}$ .  $TTT_{\mathbf{h}} = \min\{TTT(\mathbf{x}) | \mathbf{x} \in \Omega_{\mathbf{h}}\}$  represents the minimum TTT if we set the headway variable  $\mathbf{h}$  as an exogenous input. We define the minimum total travel time and optimal headway as follows:

- *Minimum total travel time (minimum TTT).*  $TTT^*$  is the minimum total travel time if  $TTT^* = \min\{TTT_{\mathbf{h}} | h_{i,j}^{\min} \leq h_{i,j}(k) \leq h_{i,j}^{\max}, (i, j) \in E \setminus (L_R \cup L_S); 1 \leq k \leq N\}$ .
- *Optimal headway.*  $\mathbf{h}$  is the optimal headway if  $TTT_{\mathbf{h}} = TTT^*$ ;  $\mathbf{h}$  and  $\mathbf{x}$  is the optimal solution of SO-DTA problem if  $\mathbf{x} \in \{\mathbf{x} | TTT(\mathbf{x}) = TTT_{\mathbf{h}} = TTT^*; \mathbf{x} \in \Omega_{\mathbf{h}}\}$ .

The proof of feasibility for the discretized form is similar that for the continuous form, and hence the detailed proof is omitted. The proposed problem is a nonlinear integer programming due to Equation 23 to 24 and Equation 26 to 27. However, if we set the headway variable  $\mathbf{h}$  as an exogenous input, the problem would become a mixed integer linear programming (MILP) in Appendix E.1. The corresponding sensitivity-based solution algorithm is presented in Appendix E.2.

However, for the SO-DTA problem, sensitivity analysis approach has large computation cost and it is hard to guarantee the convergence to global optimal solution. Proposition 4 states that the minimum TTT can be achieved under the minimum headway setting, providing us a direct way to reach the state of SO-DTA. On top of that, Proposition 5 states that it is possible to have multiple AV headway settings that yield the same SO-DTA conditions.

**Proposition 4** (Minimum headway achieves SO-DTA). *Supposing that  $\mathbf{h}^{\min} = \{h_{i,j}(k) = h_{i,j}^{\min} | (i, j) \in E \setminus (L_R \cup L_S); 1 \leq k \leq N\}$ , for  $\forall \mathbf{h}$  satisfies Equation 39, we have*

$$TTT_{\mathbf{h}^{\min}} = TTT^* \leq TTT_{\mathbf{h}}.$$

*Proof sketch.* For any feasible solution  $\mathbf{x}$  and  $\mathbf{h}$  of the proposed SO-DTA formulation, we only change a smaller  $h_{i,j}(k)$  in  $\mathbf{h}$  and keep all other headway in  $\mathbf{h}$  unchanged. The new headway is denoted as  $\mathbf{h}^*$ . Then we prove that we could always find a feasible  $\mathbf{x}^*$  under  $\mathbf{h}^*$  and the total travel time of  $\mathbf{x}^*$  is less than or equal to the total travel time of  $\mathbf{x}$  under original headway  $\mathbf{h}$ . When we traverse all links and time intervals, it is proved that SO-DTA could be achieved under the minimum headway. Details are presented in Appendix F.  $\square$

**Proposition 5** (Non-uniqueness).

$$\forall \mathbf{h} \text{ s.t. } TTT_{\mathbf{h}} = TTT^*, \text{ if } \exists \mathbf{x} \in \Omega_{\mathbf{h}} \text{ s.t. } TTT(\mathbf{x}) = TTT_{\mathbf{h}} = TTT^* \text{ and } \exists \delta_{i,j}(k) \in \mathbf{x} \text{ s.t. } \delta_{i,j}(k) = 0 \\ \text{ then } \exists \mathbf{h}^1 \neq \mathbf{h} \text{ s.t. } \mathbf{x} \in \Omega_{\mathbf{h}^1} \text{ and } TTT_{\mathbf{h}^1} = TTT(\mathbf{x}) = TTT_{\mathbf{h}} = TTT^*.$$

*Proof.* See [Appendix G](#). □

Proposition 4 aligns with Observation 1, and Proposition 5 proves Observation 2. Then we have two natural questions arise:

- If we decide to control AVs with minimum headway in reality, would it cause other concerns (e.g.. safety)?
- Is there a “best” headway among all the optimal headway given the non-uniqueness of SO-DTA solutions?

Both questions motivate us to search for a better headway control setting that still achieve the SO-DTA, which is presented in the following section.

## 5. Maximin headway control

In this section, we define the maximin headway as the “largest” headway setting among all the optimal headway setting that achieve the SO-DTA. The problem of maximin headway control is formulated and solved analytically.

### 5.1. Maximin headway control formulation

We first rigorously define the maximin headway in Definition 3.

**Definition 3** (Maximin Headway).  $\mathbf{h}^*$  is called the maximin headway if it satisfies the following two conditions:

- SO-DTA:  $TTT_{\mathbf{h}^*} = TTT^*$ , meaning that  $\mathbf{h}^*$  is the optimal headway for SO-DTA.
- Largest headway:  $\forall \mathbf{h} \text{ s.t. } TTT_{\mathbf{h}} = TTT^*$ , we have  $\|\mathbf{h}\|_1 \leq \|\mathbf{h}^*\|_1$ , where  $\|\cdot\|_1$  is the 1-norm.

Definition 3 aligns with Definition 1 with more rigor and mathematical details. We formulate a bi-level optimization to search for the maximin headway, as shown in Equation 40.

$$\begin{aligned} \max_{\mathbf{h}} \quad & \mathbf{1}^T \mathbf{h} \\ \text{s.t.} \quad & \mathbf{h} \in \left\{ \arg \min_{\mathbf{x}, \mathbf{h}} TTT \text{ (22)} \right\} \\ & \text{s.t. Headway-dependent fundamental diagram constraints (23) – (27)} \\ & \text{Headway-dependent double queue constraints (28) – (33)} \\ & \text{Flow conservation constraints (34)} \\ & \text{Non-negative Constraints (35)} \\ & \text{Initial condition constraints (36)} \\ & \text{Initial condition constraints (37)} \\ & \text{Other constraints (38) – (39)} \end{aligned} \tag{40}$$

We note it is a direct extension to replace  $\mathbf{1}^T$  with a weight vector  $\mathbf{w}^T$  to represent the importance of headway on different roads. Proposition 6 discusses the uniqueness of maximin headway of Formulation 40.

**Proposition 6** (Uniqueness of maximin headway). Suppose  $\Phi = \bigcup_{\mathbf{h}} \Omega_{\mathbf{h}}$  is the set of feasible traffic dynamics  $\mathbf{x}$ ,

$$\begin{aligned} & \text{If } \exists \mathbf{x}^* \in \Phi \text{ s.t. } TTT(\mathbf{x}^*) < TTT(\mathbf{x}), \text{ for } \forall \mathbf{x} \in \Phi \text{ and } \mathbf{x} \neq \mathbf{x}^*, \\ & \text{then } \exists \mathbf{h}^* \text{ satisfying } TTT_{\mathbf{h}^*} = TTT(\mathbf{x}^*), \text{ we have } \|\mathbf{h}^*\|_1 > \|\mathbf{h}\|_1, \forall \mathbf{h} \text{ satisfying } TTT_{\mathbf{h}} = TTT(\mathbf{x}^*) \text{ and } \mathbf{h}^* \neq \mathbf{h}. \\ & \iff \text{If } \mathbf{x}^* \text{ with } TTT(\mathbf{x}^*) = TTT^* \text{ is unique, the optimal solution of Formulation 40 is unique.} \end{aligned}$$

*Proof.* See [Appendix H](#). □

## 5.2. Maximin headway control solution algorithm

This section proposes a maximin headway control solving algorithm with the idea of exploring the maximum increase of headway to maintain the states of SO-DTA achieved by minimum headway setting. Proposition 7 provides us a method to derive a “larger” optimal headway given the current optimal headway.

**Proposition 7** (Larger headway for SO-DTA). *Suppose  $\mathbf{h}^*$  satisfies Equation 39 and  $\mathbf{x}^* \in \Omega_{\mathbf{h}^*}$  s.t.  $TTT(\mathbf{x}^*) = TTT_{\mathbf{h}^*} = TTT^*$ . If  $\mathbf{h}$  satisfies following constraints:*

$$\begin{aligned}
 & \text{if } \delta_{i,j}^*(k) = 0 : \\
 & \quad \rho_{i,j}^*(k) v_{i,j}^f h_{i,j}(k) < 1 - \rho_{i,j}^*(k) L \\
 & \quad L_{i,j} h_{i,j}(k) \geq \Delta_t L n_{i,j}^{w,*}(k) \\
 & \quad L_{i,j} h_{i,j}(k) < \Delta_t L n_{i,j}^{w,*}(k) + \Delta_t L \\
 & \quad h_{i,j}^*(k) < h_{i,j}(k) \leq h_{i,j}^{max} \\
 & \text{if } \delta_{i,j}^*(k) = 1 : \\
 & \quad h_{i,j}(k) = h_{i,j}^*(k),
 \end{aligned}$$

where  $\delta_{i,j}^*(k)$ ,  $\rho_{i,j}^*(k)$  and  $n_{i,j}^{w,*}(k) \in \mathbf{x}^*$ , then we have  $\mathbf{x}^* \in \Omega_{\mathbf{h}}$ ,  $TTT_{\mathbf{h}} = TTT(\mathbf{x}^*) = TTT^*$  and  $\|\mathbf{h}^*\|_1 < \|\mathbf{h}\|_1$ .

*Proof.* See Appendix I. □

Proposition 4 and 7 inspire us a way to derive the maximin headway control and it mainly consists of the following two steps: 1) derive the flow dynamics  $\mathbf{x}^*$  for SO-DTA under the minimum headway  $\mathbf{h}^{min}$ ; 2) explore the “largest” headway setting based on  $\mathbf{x}^*$  by remaining the same TTT.

To this end, we propose an algorithm to solve the maximin headway control in Algorithm 1 and prove the correctness of Algorithm 1 under the condition of the existence of unique optimal flow dynamics in Proposition 8. One can see from Algorithm 1 that, once the traffic condition  $\mathbf{x}^*$  is determined, we can run a linear programming (LP) to solve for the maximin headway, and hence the solution process is computationally efficient.

---

### Algorithm 1 Maximin Headway Control Solving Algorithm

---

**Input:** parameters in Table A.4.

- 1: Solve the discretized SO-DTA formulation (Equations 22 to 38) under minimum headway  $\mathbf{h}^{min}$  to derive the optimal flow dynamics  $\mathbf{x}^*$  with  $TTT(\mathbf{x}^*) = TTT_{\mathbf{h}^{min}} = TTT^*$ . To be specific, we can solve Formulation 41 to obtain  $\mathbf{x}^*$ , and details of the formulation is presented in Appendix E.1.

$$\begin{aligned}
 \mathbf{x}^* &= \arg \min_{\mathbf{x}} TTT = \mathbf{P}^T \mathbf{x} \\
 \text{s.t.} \quad & \mathbf{A}(\mathbf{h}^{min}) \mathbf{x} = \mathbf{B}(\mathbf{h}^{min}) \\
 & \mathbf{C}(\mathbf{h}^{min}) \mathbf{x} \leq \mathbf{D}(\mathbf{h}^{min})
 \end{aligned} \tag{41}$$

- 2: Solve Formulation 42 under the flow dynamics  $\mathbf{x}^*$  and derive the maximin headway  $\mathbf{h}^*$ , where  $\delta_{i,j}^*(k)$ ,  $\rho_{i,j}^*(k)$  and  $n_{i,j}^{w,*}(k) \in \mathbf{x}^*$ .

$$\begin{aligned}
 & \max_{\mathbf{h}} \mathbf{1}^T \mathbf{h} \\
 \text{s.t.} \quad & \text{if } \delta_{i,j}^*(k) = 0 : \\
 & \quad \rho_{i,j}^*(k) v_{i,j}^f h_{i,j}(k) < 1 - \rho_{i,j}^*(k) L \\
 & \quad L_{i,j} h_{i,j}(k) \geq \Delta_t L n_{i,j}^{w,*}(k) \\
 & \quad L_{i,j} h_{i,j}(k) < \Delta_t L n_{i,j}^{w,*}(k) + \Delta_t L \\
 & \quad h_{i,j}^{min}(k) < h_{i,j}(k) \leq h_{i,j}^{max} \\
 & \text{if } \delta_{i,j}^*(k) = 1 : \\
 & \quad h_{i,j}(k) = h_{i,j}^{min}(k)
 \end{aligned} \tag{42}$$

**Output:** maximin headway  $\mathbf{h}^*$  and optimal flow dynamics  $\mathbf{x}^*$  with  $\mathbf{x}^* \in \Omega_{\mathbf{h}^*}$  and  $TTT_{\mathbf{h}^*} = TTT(\mathbf{x}^*) = TTT^*$ .

**Proposition 8** (Correctness of Algorithm 1). *The output  $\mathbf{h}^*$  of Algorithm 1 is the optimal solution of Formulation 40 if  $\exists \mathbf{x}^* \in \Phi$  s.t.  $TTT(\mathbf{x}^*) < TTT(\mathbf{x}), \forall \mathbf{x} \in \Phi$  and  $\forall \mathbf{x} \neq \mathbf{x}^*$ .*

*Proof.* Proposition 8 can be directly obtained by combining Proposition 4, 6, and 7.  $\square$

## 6. Numerical experiments

The proposed model and propositions are validated on both a small and a large-scale network in this section.

### 6.1. A small network

In the small network, we first solve for the optimal headway control and maximin headway control to demonstrate that the maximin headway control achieves the SO-DTA with large headway settings. Additionally, the sensitivity analysis for the maximin headway control is also conducted.

#### 6.1.1. Settings

The small network consists of 5 nodes and 6 links, Node 1 and 2 are connected to the origins and Node 5 is connected with the destination. The minimum and maximum headway in each link are set as 0.5 seconds and 2.5 seconds, respectively. We further set the total time horizon  $T$  as 90 minutes and the length of each time interval  $\Delta_t$  as 5 minutes. The travel demand for each O-D pair is 50 *vehicles/mins* and the time horizon of demand  $T_1$  is 40 minutes. Other parameters are illustrated in Appendix J.

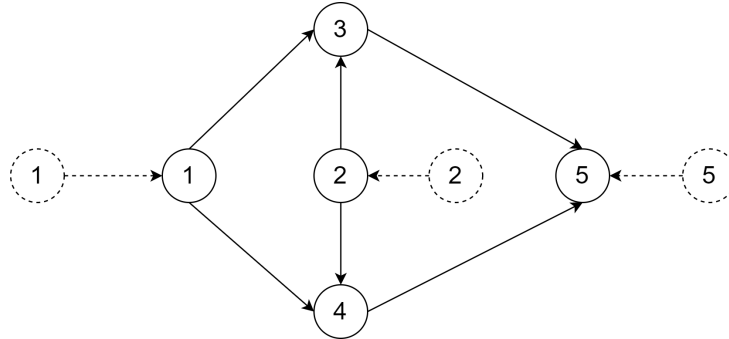


Figure 4: The small network.

#### 6.1.2. Results for optimal and maximin headway control

The three different scenarios are defined for comparison as follows:

- **Min-HW:** the headway of each link is directly set as the minimum headway.
- **SO-HW:** we directly solve for the SO-DTA by searching for the optimal headway, and the solution algorithm is based on the sensitivity-based algorithm (Algorithm 2) described in Appendix E.2.
- **Maximin-HW:** we solve the maximin headway by Algorithm 1.

Based on Proposition 4, we already know that the minimum headway setting would yield the SO-DTA, and the total travel time  $TTT(\mathbf{h}^{min}) = 27,740$ . Additionally, the dynamic inflow and outflow of each link in the SO-DTA are presented in Figure 5.

The convergence curve of Algorithm 2 in SO-HW is shown in Figure 6, and one can see that the algorithm converges to about  $TTT = 33,500$  minutes, which is larger than 27,740 derived by Algorithm 1 in Minimum-HW. This verifies that the Min-HW has lower TTT than SO-HW, and the sensitivity-based method might not converge to the optimal solution of SO-DTA.

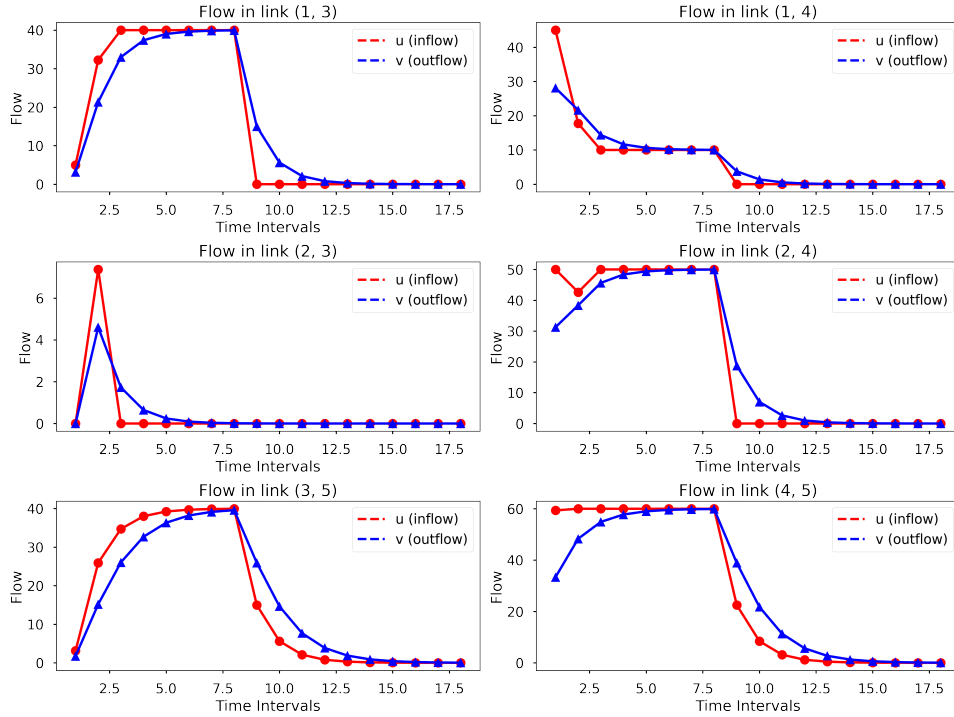


Figure 5: Inflow and outflow of each link under SO-DTA.

As for the **Maximin-HW**, the TTT remains 27,740 minutes, meaning that the maximin headway still achieves the SO-DTA. More importantly, the maximin headway is about 2.42 times as large as the minimum headway on average, demonstrating the merits of the maximin headway control. Table 3 presents the average maximin headway and minimum headway of each link. One can see that the gap between the maximin and minimum headway is significant, and the gap could also reflect the safety margin of each link.

Link	Minimum Headway (seconds)	Maximin Headway (seconds)
1 → 3	0.500	0.994
1 → 4	0.500	1.050
2 → 3	0.500	2.500
2 → 4	0.500	0.962
3 → 5	0.500	0.944
4 → 5	0.500	0.804

Table 3: Maximin and minimum headway in the small network.

### 6.1.3. Sensitivity analysis for the maximin headway control

This section explores how different network configurations would effect the average gap between the maximin headway control and minimum headway control and it could be formulated as  $\frac{\|\mathbf{h}^* - \mathbf{h}^{min}\|_1}{n_L N}$ , where  $\mathbf{h}^*$  is the maximin headway solved by Algorithm 1 and  $n_L$  is the number of links in set  $E \setminus (L_R \cup L_S)$ . In particular, we study the sensitivity regarding the travel demand and minimum headway.

**Travel demand.** We first conduct the sensitivity analysis regarding travel demand under different minimum headway requirements. We vary the demand of each O-D pair from 30 to 70 under different minimum headway



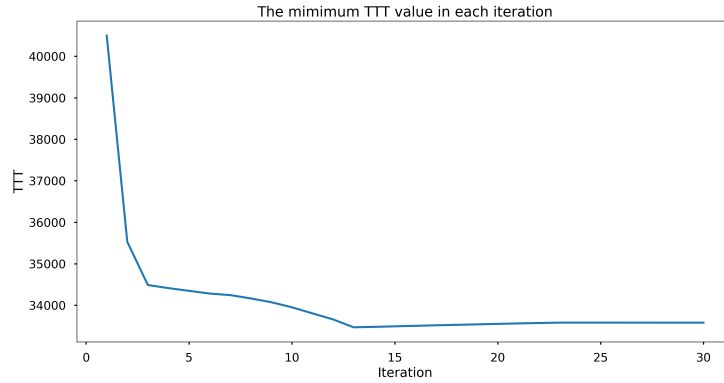


Figure 6: Convergence curve in terms of TTT by Algorithm 2.

requirements, then we solve Algorithm 1 and derive the value of the average gap between the maximum headway and minimum headway, and the results are shown in Figure 7.

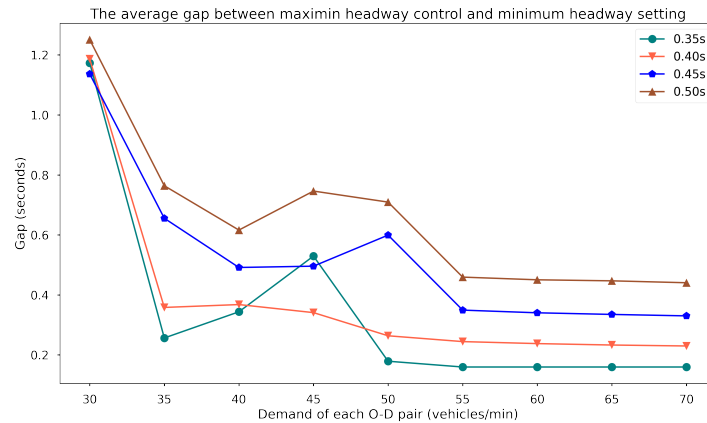


Figure 7: The average gap between the maximum and minimum headway under different traffic demand.

One can see that the average gap between maximum and minimum headway settings decreases when the demand increases, indicating that the safety margin for SO-DTA will become marginal when more people travel.

**Minimum headway.** Then the sensitivity analysis for the minimum headway value is conducted. We vary the value of minimum headway from 0.20s to 1.10s under different O-D demand and keep other parameters unchanged. Then we solve the Algorithm 1 and derive the value of the average gap between the maximum headway control and minimum headway setting under different minimum headway values. Figure 8 shows how the average gap between the maximum headway control and minimum headway setting would change corresponding to different minimum headway values.

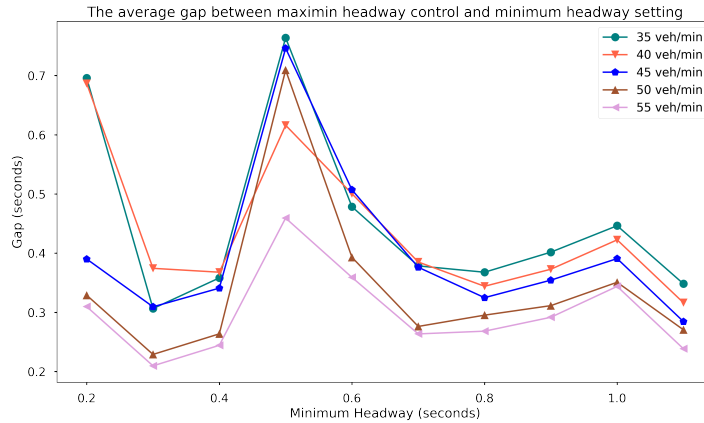


Figure 8: The average gap between the maximin and minimum headway under different minimum headway settings.

One can see that in general, the average headway gap between maximin and minimum headway is relatively stabilized under different minimum headway, indicating that there is always room to enlarge the headway after achieving SO-DTA under different safety requirements (*i.e.*, minimum headway).

## 6.2. Sioux Falls network

In this section, we solve for the maximin headway control on the Sioux Falls network.

### 6.2.1. Settings

The Sioux Falls network consists of 24 nodes and 76 links, and the detailed network settings, such as link length and capacity, can be referred to the website<sup>1</sup>. Besides, we further define that the minimum and maximum headway in each link are set as 0.5 seconds and 2.5 seconds, respectively.

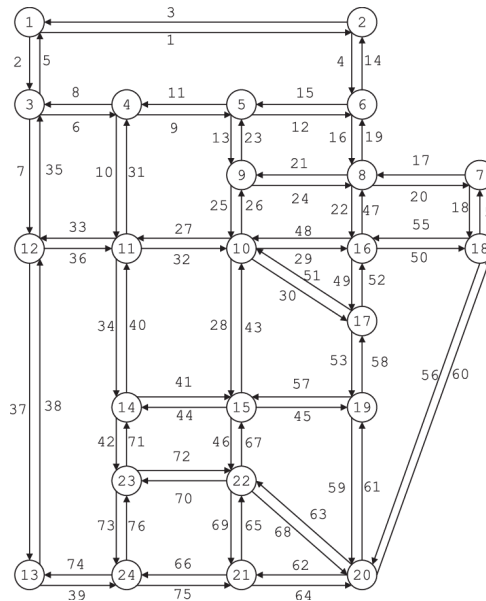


Figure 9: Overview of the Sioux Falls network.

<sup>1</sup><https://github.com/bstabler/TransportationNetworks/tree/master/SiouxFalls>

### 6.2.2. Experimental results

We consider **Min-HW** and **Maximin-HW** by setting the minimum headway directly and running Algorithm 1, respectively. **SO-HW** is omitted as we have already proved that **Min-HW** is equivalent to **SO-HW**. Details of **Min-HW** and **Maximin-HW** are presented as follows:

- **Min-HW**: we directly set the minimum headway for each link, and we have  $TTT(\mathbf{h}_{min}) = 23,674$  minutes.
- **Maximin-HW**: The  $TTT$  is the same as that of the **Min-HW**, and the average gap between the maximin headway and the minimum headway is 1.045 seconds. On average, each headway setting in maximin headway control is about 3.09 times as large as the minimum headway.

## 7. Conclusion

In this paper, we propose a maximin headway control framework for SO-DTA on general networks in a fully automated environment. Both HFD and HDQ are developed to capture effects of dynamic AV headway control. Particularly, the HDQ is proved to be a generalized version of the DQ. It is rigorously proved that the minimum headway could achieve SO-DTA. On top of this, the maximin headway of AVs is innovatively defined as the “largest” headway setting that still achieves SO-DTA. We further propose an efficient solution algorithm to derive the maximin headway. Numerical experiments demonstrate the correctness and effectiveness of the proposed framework. Sensitivity analysis demonstrates that the increase in travel demand would normally correspond to a decrease in gap values between the maximin and minimum headway, which helps the policymakers understand the safety margin of AVs on different links. We believe this study provides novel angles and mathematical techniques to derive and analyze the “desired solution” among the non-unique solutions in SO-DTA.

Future studies can be conducted to consider mixed traffic conditions, heterogeneous travel behaviors, and stochastic traffic demand and road supply. For example, this study is based on the HFD and HDQ in a fully automated environment so that we could control the headway of all AVs for SO-DTA. However, in mixed traffic conditions, the route choice of human-driving vehicles (HVs) may follow dynamic user equilibrium (DUE), making the problem more complex (Zhang & Nie 2018). It is also interesting to explore the headway control on a limited number of roads or with limited control capacities (Battifarano & Qian 2023). Additionally, quantifying the relationship between headway and safety is critical to the practical deployment of the developed headway control framework in the real world.

## Acknowledgments

The work described in this paper was supported by the National Natural Science Foundation of China (No. 52102385), a grant from the Research Grants Council of the Hong Kong Special Administrative Region, China (Project No. PolyU/25209221), and grants from the Otto Poon Charitable Foundation Smart Cities Research Institute (SCRI) at the Hong Kong Polytechnic University (Project No. P0043552 & P0036472).

## References

- Bagloee, S., Sarvi, M., Patriksson, M. & Rajabifard, A. (2017), ‘A mixed user-equilibrium and system-optimal traffic flow for connected vehicles stated as a complementarity problem: Mixed user-equilibrium and system-optimal traffic flow’, *Computer-Aided Civil and Infrastructure Engineering* **32**.
- Battifarano, M. & Qian, S. (2023), ‘The impact of optimized fleets in transportation networks’, *Transportation Science*.
- Chen, Z., He, F., Yin, Y. & Du, Y. (2017), ‘Optimal design of autonomous vehicle zones in transportation networks’, *Transportation Research Part B: Methodological* **99**, 44–61.
- Chen, Z., He, F., Zhang, L. & Yin, Y. (2016), ‘Optimal deployment of autonomous vehicle lanes with endogenous market penetration’, *Transportation Research Part C: Emerging Technologies* **72**, 143–156.

- Chiu, Y.-C., Zheng, H., Villalobos, J. & Gautam, B. (2007), 'Modeling no-notice mass evacuation using a dynamic traffic flow optimization model', *Iie Transactions* **39**(1), 83–94.
- Chow, A. H. (2009), 'Properties of system optimal traffic assignment with departure time choice and its solution method', *Transportation Research Part B: Methodological* **43**(3), 325–344.
- Daganzo, C. F. (1995), 'The cell transmission model, part ii: Network traffic', *Transportation Research Part B: Methodological* **29**(2), 79–93.
- Gawron, C. (1998), 'An iterative algorithm to determine the dynamic user equilibrium in a traffic simulation model', *International Journal of Modern Physics C* **9**(03), 393–407.
- Gong, S., Shen, J. & Du, L. (2016), 'Constrained optimization and distributed computation based car following control of a connected and autonomous vehicle platoon', *Transportation Research Part B: Methodological* **94**, 314–334.
- Guo, Q. & Ban, X. (2020), 'Macroscopic fundamental diagram based perimeter control considering dynamic user equilibrium', *Transportation Research Part B: Methodological* **136**, 87–109.
- Han, K., Liu, H., Gayah, V. V., Friesz, T. L. & Yao, T. (2016), 'A robust optimization approach for dynamic traffic signal control with emission considerations', *Transportation Research Part C: Emerging Technologies* **70**, 3–26.
- Hatipoglu, C., Ozguner, U. & Sommerville, M. (1996), Longitudinal headway control of autonomous vehicles, *in* 'Proceeding of the 1996 IEEE International Conference on Control Applications IEEE International Conference on Control Applications held together with IEEE International Symposium on Intelligent Control', IEEE, pp. 721–726.
- Levin, M. W. (2017), 'Congestion-aware system optimal route choice for shared autonomous vehicles', *Transportation Research Part C: Emerging Technologies* **82**, 229–247.
- Levin, M. W. (2019), 'Linear program for system optimal parking reservation assignment', *Journal of Transportation Engineering, Part A: Systems* **145**(12), 04019049.
- Levin, M. W. & Boyles, S. D. (2016), 'A multiclass cell transmission model for shared human and autonomous vehicle roads', *Transportation Research Part C: Emerging Technologies* **62**, 103–116.
- Li, L. & Chen, X. M. (2017), 'Vehicle headway modeling and its inferences in macroscopic/microscopic traffic flow theory: A survey', *Transportation Research Part C: Emerging Technologies* **76**, 170–188.
- Li, X. (2022), 'Trade-off between safety, mobility and stability in automated vehicle following control: An analytical method', *Transportation research part B: methodological* **166**, 1–18.
- Liu, J., Mirchandani, P. & Zhou, X. (2020), 'Integrated vehicle assignment and routing for system-optimal shared mobility planning with endogenous road congestion', *Transportation Research Part C: Emerging Technologies* **117**, 102675.
- Liu, Y., Lai, X. & Chang, G.-L. (2006), 'Cell-based network optimization model for staged evacuation planning under emergencies', *Transportation Research Record* **1964**(1), 127–135.
- Lo, H. K. (2001), 'A cell-based traffic control formulation: strategies and benefits of dynamic timing plans', *Transportation Science* **35**(2), 148–164.
- Long, J., Chen, J., Szeto, W. & Shi, Q. (2018), 'Link-based system optimum dynamic traffic assignment problems with environmental objectives', *Transportation Research Part D: Transport and Environment* **60**, 56–75.
- Long, J. & Szeto, W. Y. (2019), 'Link-based system optimum dynamic traffic assignment problems in general networks', *Operations Research* **67**(1), 167–182.
- Lu, C.-C., Liu, J., Qu, Y., Peeta, S., Roupail, N. M. & Zhou, X. (2016), 'Eco-system optimal time-dependent flow assignment in a congested network', *Transportation Research Part B: Methodological* **94**, 217–239.

- Ma, R., Ban, X. J. & Pang, J.-S. (2014), ‘Continuous-time dynamic system optimum for single-destination traffic networks with queue spillbacks’, *Transportation Research Part B: Methodological* **68**, 98–122.
- Ma, R., Ban, X. J. & Szeto, W. (2017), ‘Emission modeling and pricing on single-destination dynamic traffic networks’, *Transportation Research Part B: Methodological* **100**, 255–283.
- Ngoduy, D., Hoang, N., Vu, H. L. & Watling, D. (2016), ‘Optimal queue placement in dynamic system optimum solutions for single origin-destination traffic networks’, *Transportation Research Part B: Methodological* **92**, 148–169.
- Ngoduy, D., Hoang, N., Vu, H. & Watling, D. (2021), ‘Multiclass dynamic system optimum solution for mixed traffic of human-driven and automated vehicles considering physical queues’, *Transportation Research Part B: Methodological* **145**, 56–79.
- Nguyen, C. H., Hoang, N. H., Lee, S. & Vu, H. L. (2021), ‘A system optimal speed advisory framework for a network of connected and autonomous vehicles’, *IEEE Transactions on Intelligent Transportation Systems* **23**(6), 5727–5739.
- Osorio, C., Flötteröd, G. & Bierlaire, M. (2011), ‘Dynamic network loading: a stochastic differentiable model that derives link state distributions’, *Procedia-Social and Behavioral Sciences* **17**, 364–381.
- Penrose, R. (1955), A generalized inverse for matrices, in ‘Mathematical proceedings of the Cambridge philosophical society’, Vol. 51, Cambridge University Press, pp. 406–413.
- Qian, Z. S. & Rajagopal, R. (2014), ‘Optimal dynamic parking pricing for morning commute considering expected cruising time’, *Transportation Research Part C: Emerging Technologies* **48**, 468–490.
- Qian, Z. S., Shen, W. & Zhang, H. (2012), ‘System-optimal dynamic traffic assignment with and without queue spillback: Its path-based formulation and solution via approximate path marginal cost’, *Transportation research part B: methodological* **46**(7), 874–893.
- Samaranayake, S., Krichene, W., Reilly, J., Monache, M. L. D., Goatin, P. & Bayen, A. (2018), ‘Discrete-time system optimal dynamic traffic assignment (so-dta) with partial control for physical queuing networks’, *Transportation Science* **52**(4), 982–1001.
- Seo, T. & Asakura, Y. (2022), ‘Multi-objective linear optimization problem for strategic planning of shared autonomous vehicle operation and infrastructure design’, *IEEE Transactions on Intelligent Transportation Systems* **23**(4), 3816–3828.
- Shen, W. & Zhang, H. (2014), ‘System optimal dynamic traffic assignment: Properties and solution procedures in the case of a many-to-one network’, *Transportation Research Part B: Methodological* **65**, 1–17.
- Shi, X. & Li, X. (2021), ‘Constructing a fundamental diagram for traffic flow with automated vehicles: Methodology and demonstration’, *Transportation Research Part B: Methodological* **150**, 279–292.
- Szeto, W. & Lo, H. K. (2006), ‘Dynamic traffic assignment: properties and extensions’, *Transportmetrica* **2**(1), 31–52.
- Tan, Y., Ma, R., Sun, Z. & Zhang, P. (2021), ‘Emission exposure optimum for a single-destination dynamic traffic network’, *Transportation Research Part D: Transport and Environment* **94**, 102817.
- van Essen, M., Thomas, T., van Berkum, E. & Chorus, C. (2016), ‘From user equilibrium to system optimum: a literature review on the role of travel information, bounded rationality and non-selfish behaviour at the network and individual levels’, *Transport reviews* **36**(4), 527–548.
- Wadud, Z., MacKenzie, D. & Leiby, P. (2016), ‘Help or hindrance? the travel, energy and carbon impacts of highly automated vehicles’, *Transportation Research Part A: Policy and Practice* **86**, 1–18.

- Waller, S. T., Mouskos, K. C., Kamaryiannis, D. & Ziliaskopoulos, A. K. (2006), 'A linear model for the continuous network design problem', *Computer-Aided Civil and Infrastructure Engineering* **21**(5), 334–345.
- Waller, S. T. & Ziliaskopoulos, A. K. (2001), 'Stochastic dynamic network design problem', *Transportation Research Record* **1771**(1), 106–113.
- Wang, G., Qi, H., Xu, H. & Ryu, S. (2020), 'A mixed behaviour equilibrium model with mode choice and its application to the endogenous demand of automated vehicles', *Journal of Management Science and Engineering* **5**(4), 227–248. Special Issue on Traffic and Transportation in the Era of Big Data and Shared Economy.
- Wang, J., Peeta, S. & He, X. (2019), 'Multiclass traffic assignment model for mixed traffic flow of human-driven vehicles and connected and autonomous vehicles', *Transportation Research Part B: Methodological* **126**, 139–168.
- Wang, Y., Szeto, W. Y., Han, K. & Friesz, T. L. (2018), 'Dynamic traffic assignment: A review of the methodological advances for environmentally sustainable road transportation applications', *Transportation Research Part B: Methodological* **111**, 370–394.
- Wardrop, J. G. (1952), 'Road paper. some theoretical aspects of road traffic research.', *Proceedings of the institution of civil engineers* **1**(3), 325–362.
- Yperman, I. (2007), 'The link transmission model for dynamic network loading'.
- Yu, H., Jiang, R., He, Z., Zheng, Z., Li, L., Liu, R. & Chen, X. (2021), 'Automated vehicle-involved traffic flow studies: A survey of assumptions, models, speculations, and perspectives', *Transportation Research Part C: Emerging Technologies* **127**, 103101.
- Zhang, K. & Nie, Y. M. (2018), 'Mitigating the impact of selfish routing: An optimal-ratio control scheme (orcs) inspired by autonomous driving', *Transportation Research Part C: Emerging Technologies* **87**, 75–90.
- Zhang, P. & Qian, S. (2020), 'Path-based system optimal dynamic traffic assignment: A subgradient approach', *Transportation Research Part B: Methodological* **134**, 41–63.
- Zhou, J. & Zhu, F. (2020), 'Modeling the fundamental diagram of mixed human-driven and connected automated vehicles', *Transportation Research Part C: Emerging Technologies* **115**, 102614.

## Appendix A. Notations

Type	Notation	Description	
Sets	$V$	Set of nodes	
	$R$	Set of origins	
	$\bar{R}$	Set of dummy origins	
	$S$	Set of destinations	
	$\bar{S}$	Set of dummy destinations	
	$E$	Set of links	
	$L_R$	Set of origin connectors	
	$L_S$	Set of destination connectors	
	Parameters	$v_{i,j}^f$	Free-flow speed of link $(i, j)$
		$L_{i,j}$	Length of link $(i, j)$
$L$		Length of an AV	
$\bar{Q}_{i,j}^u$		Upstream queue capacity of link $(i, j)$	
$\bar{Q}_{i,j}^d$		Downstream queue capacity of link $(i, j)$	
$\bar{C}_{i,j}^u$		Inflow capacity of link $(i, j)$	
$\bar{C}_{i,j}^v$		Outflow capacity of link $(i, j)$	
$T_I$		Time horizon of demand	
$T$		Total time horizon	
$h_{i,j}^{\min}$		Lower bound of headway in link $(i, j)$	
$h_{i,j}^{\max}$		Upper bound of headway in link $(i, j)$	
Variables		$u_{i,j}(t)$	Inflow of the flow area of link $(i, j)$ at time $t$
		$u_{i,j}^{s'}(t)$	Inflow of the flow area of link $(i, j)$ with destination $s'$ at time $t$
	$v_{i,j}(t)$	Outflow of the buffer area of link $(i, j)$ at time $t$	
	$v_{i,j}^{s'}(t)$	Outflow of the buffer area of link $(i, j)$ with destination $s'$ at time $t$	
	$f_{i,j}(t)$	Inflow at the boundary of the flow area and buffer area of link $(i, j)$ at time $t$	
	$f_{i,j}^{s'}(t)$	Inflow at the boundary of the flow area and buffer area of link $(i, j)$ with destination $s'$ at time $t$	
	$\rho_{i,j}(t)$	Density of the flow area of link $(i, j)$ at time $t$	
	$\rho_{i,j}^{s'}(t)$	Density of the flow area of link $(i, j)$ with destination $s'$ at time $t$	
	$q_{i,j}^d(t)$	Downstream queue of link $(i, j)$ at time $t$	
	$q_{i,j}^{d,s'}(t)$	Downstream queue of link $(i, j)$ with destination $s'$ at time $t$	
	$q_{i,j}^u(t)$	Upstream queue of link $(i, j)$ at time $t$	
	$q_{i,j}^{u,s'}(t)$	Upstream queue of link $(i, j)$ with destination $s'$ at time $t$	
	$h_{i,j}(t)$	Headway of automated vehicles in link $(i, j)$ at time $t$	
	$\tau_{i,j}^w(t)$	Shockwave travel time on link $(i, j)$ at time $t$	
	$d_{r',s'}(t)$	Travel demand of O-D pair $(r', s')$ at time $t$	
	$U_{i,j}(t)$	Cumulative inflow of the flow area of link $(i, j)$ at time $t$	
	$F_{i,j}(t)$	Cumulative inflow at the boundary of the flow area and buffer area of link $(i, j)$ at time $t$	
	$V_{i,j}(t)$	Cumulative outflow of the buffer area of link $(i, j)$ at time $t$	

Table A.4: Notation table.

## Appendix B. Proof of Proposition 1

Proposition 1 indicates that the headway-dependent double queue (HDQ) model is a generalized form of the double queue (DQ) model. The formulation of the downstream queue  $q_{i,j}^d(t)$  and upstream queue  $q_{i,j}^u(t)$  in DQ for  $(i, j) \in E$  and  $t \in [0, T]$  are shown as follows:

$$\begin{aligned}
 q_{i,j}^d(t) &= \int_0^{t-\tau_{i,j}^f} u_{i,j}(t) dt - \int_0^t v_{i,j}(t) dt + q_{i,j}^d(0) = U_{i,j}(t - \tau_{i,j}^f) - V_{i,j}(t), \\
 q_{i,j}^u(t) &= \int_0^t u_{i,j}(t) dt - \int_0^{t-\tau_{i,j}^w} v_{i,j}(t) dt + q_{i,j}^u(0) = U_{i,j}(t) - V_{i,j}(t - \tau_{i,j}^w),
 \end{aligned}$$

where  $q_{i,j}^d(t)$  and  $q_{i,j}^u(t)$  represent the downstream and upstream queue in link  $(i, j)$  at time  $t$  in DQ, respectively, and the two queues are interpreted as follows:

- Downstream queue  $q_{i,j}^d(t)$  measures the number of vehicles at the end of link  $(i, j)$  at time  $t$ . DQ assumes the inflow  $u_{i,j}$  would travel from the entrance to the end of link  $(i, j)$  at the free-flow speed, and the outflow of link  $(i, j)$  at time  $t$  is determined by the outflow capacity link  $(i, j)$  and upstream queue in next link.
- Upstream queue  $q_{i,j}^u(t)$  measures the number of vehicles at the entrance of link  $(i, j)$  at time  $t$ . DQ assumes the space of outflow  $v_{i,j}$  would travel from the end to the entrance of link  $(i, j)$  at the shockwave speed.

However, the assumptions of DQ model may have following limitations:

- Congestion may occur in the flow area of link so that AVs may not travel from the entrance to the end of link at the free-flow speed. The influence of headway on the flow of link is also not considered in DQ.
- Space may not propagate to the entrance of link in time and retain in the downstream. Take an extreme example, if the front AV leave the link but other AVs behind are still, the space left by the front AV would still retain in the downstream and it is not accurate to use the outflow to calculate the propagation of space in shockwave speed. Besides, the influence of headway on the shockwave speed on link is also not considered in DQ.

The HDQ addresses the above limitations by exploring the effects of headway. Equation 6 and 7 formulate the downstream and upstream queue in HDQ. The relationship between the HDQ and DQ are presented in Equation B.1 and B.2.

$$\begin{aligned}
q_{i,j}^d(t) &= U_{i,j}(t - \tau_{i,j}^f) - V_{i,j}(t) \\
&= U_{i,j}(t - \tau_{i,j}^f) - F_{i,j}(t) + F_{i,j}(t) - V_{i,j}(t) \\
&= q_{i,j}^D(t) + U_{i,j}(t - \tau_{i,j}^f) - F_{i,j}(t)
\end{aligned} \tag{B.1}$$

$$\begin{aligned}
q_{i,j}^u(t) &= U_{i,j}(t) - V_{i,j}(t - \tau_{i,j}^w) \\
&= U_{i,j}(t) - F_{i,j}(t - \tau_{i,j}^w) + F_{i,j}(t - \tau_{i,j}^w) - V_{i,j}(t - \tau_{i,j}^w) \\
&= q_{i,j}^U(t) + q_{i,j}^D(t - \tau_{i,j}^w)
\end{aligned} \tag{B.2}$$

In Equation B.1,  $U_{i,j}(t - \tau_{i,j}^f) - F_{i,j}(t)$  represents the congestion in the flow area in HDQ. However, under the assumption of DQ, we have  $u_{i,j}(t - \tau_{i,j}^f) = f_{i,j}(t)$ , meaning that vehicles would travel from the entrance of link to the boundary of the flow area and buffer area at free-flow speed. Therefore, the downstream queue of HDQ is equivalent to the DQ as follows:

$$q_{i,j}^d(t) = q_{i,j}^D(t) + U_{i,j}(t - \tau_{i,j}^f) - F_{i,j}(t) = q_{i,j}^D(t).$$

In Equation B.2, the upstream queue in DQ actually consists of the queue in both flow area and buffer area in HDQ. The upstream queue in HDQ actually consider the flow entering buffer area to fill the leaving space. If we ignore it, we would derive the upstream queue by outflow  $v$  as DQ.

Different from DQ, the HDQ specifies the traffic state in a link and incorporates the effect of headway. To calculate the number of AVs at the entrance and end of a link, we just focus on the flow area and buffer area, respectively. Compared with the DQ, the HDQ provides a more precise way to calculate the downstream and upstream queue if we are clear about the state of boundary of the flow area and buffer area compared with the DQ. If under the assumption of DQ, the effect of headway is ignored and HDQ would be reduced to DQ.

## Appendix C. Proof of Proposition 2

This appendix proves the properties of the headway-dependent double queue (HDQ) model, and we mainly show the constraints on the flow rates of the HDQ.



With Eqs.(4.29) in [Yperman \(2007\)](#) and the formulation of the downstream queue in HDQ, Equation C.1 presents the constraint on the sending flow  $S_{i,j}(t)$  of HDQ.

$$S_{i,j}(t) \leq V_{i,j}(t + \Delta_t) - V_{i,j}(t) \leq F_{i,j}(t + \Delta_t) - V_{i,j}(t) \quad (\text{C.1})$$

With Eqs.(4.33) in [Yperman \(2007\)](#) and the formulation of the upstream queue in HDQ, the constraint on the receiving flow  $R_{i,j}(t)$  of the HDQ is stated in Equation C.2.

$$R_{i,j}(t) \leq U_{i,j}(t + \Delta_t) - U_{i,j}(t) \leq \bar{Q}_{i,j}^u + F_{i,j}(t + \Delta_t) - \tau_{i,j}^w(t) - U_{i,j}(t) \quad (\text{C.2})$$

When the time step  $\Delta_t$  approaches zero, the constraint of outflow  $v$  is shown in C.3 and the constraint of inflow  $u$  is shown in C.4.

$$\begin{aligned} v_{i,j}(t) &\leq \lim_{\Delta_t \rightarrow 0} \frac{S_{i,j}(t)}{\Delta_t} \leq \lim_{\Delta_t \rightarrow 0} \min \left\{ \frac{F_{i,j}(t + \Delta_t) - V_{i,j}(t)}{\Delta_t}, \bar{C}_{i,j}^v \right\} \\ &= \lim_{\Delta_t \rightarrow 0} \min \left\{ \frac{F_{i,j}(t + \Delta_t) - F_{i,j}(t)}{\Delta_t} + \frac{F_{i,j}(t) - V_{i,j}(t)}{\Delta_t}, \bar{C}_{i,j}^v \right\} \\ &= \lim_{\Delta_t \rightarrow 0} \min \left\{ \frac{F_{i,j}(t + \Delta_t) - F_{i,j}(t)}{\Delta_t} + \frac{q_{i,j}^D(t)}{\Delta_t}, \bar{C}_{i,j}^v \right\} \\ &= \begin{cases} \bar{C}_{i,j}^v, & q_{i,j}^D(t) > 0 \\ \min \{f_{i,j}(t), \bar{C}_{i,j}^v\}, & q_{i,j}^D(t) = 0 \end{cases} \end{aligned} \quad (\text{C.3})$$

$$\begin{aligned} u_{i,j}(t) &\leq \lim_{\Delta_t \rightarrow 0} \frac{R_{i,j}(t)}{\Delta_t} \leq \lim_{\Delta_t \rightarrow 0} \min \left\{ \frac{\bar{Q}_{i,j}^u + F_{i,j}(t + \Delta_t) - \tau_{i,j}^w(t) - V_{i,j}(t)}{\Delta_t}, \bar{C}_{i,j}^\mu \right\} \\ &= \lim_{\Delta_t \rightarrow 0} \min \left\{ \frac{\bar{Q}_{i,j}^u - (V_{i,j}(t) - F_{i,j}(t - \tau_{i,j}^w(t)))}{\Delta_t} + \frac{F_{i,j}(t + \Delta_t) - \tau_{i,j}^w(t) - F_{i,j}(t - \tau_{i,j}^w(t))}{\Delta_t}, \bar{C}_{i,j}^\mu \right\} \\ &= \lim_{\Delta_t \rightarrow 0} \min \left\{ \frac{\bar{Q}_{i,j}^u - q_{i,j}^U(t)}{\Delta_t} + \frac{F_{i,j}(t + \Delta_t) - \tau_{i,j}^w(t) - F_{i,j}(t - \tau_{i,j}^w(t))}{\Delta_t}, \bar{C}_{i,j}^\mu \right\} \\ &= \begin{cases} \bar{C}_{i,j}^\mu, & q_{i,j}^U(t) < \bar{Q}_{i,j}^u \\ \min \{f_{i,j}(t - \tau_{i,j}^w(t)), \bar{C}_{i,j}^\mu\}, & q_{i,j}^U(t) = \bar{Q}_{i,j}^u \end{cases} \end{aligned} \quad (\text{C.4})$$

### Appendix D. Proof of Proposition 3

In general, we could construct a feasible solution to Equation 21 using the following three steps:

- Let all the demand of each O-D pair arrive at the downstream queue in the origin connectors while not releasing them. We define the time period for such a process as  $T_l$ . We don't consider the capacity of number of AVs waiting at origins here.
- For each O-D pair  $(r', s')$ , we divide the total demand  $D^{r',s'}$  into many equal batches  $B^{r',s'}$ , and  $D^{r',s'} = n^{r',s'} B^{r',s'}$ . We only use one path of each O-D pair  $(r', s')$ , which is denoted as  $P^{r',s'}$ . We only release one batch of an O-D pair only once. After all the AVs in this batch arrive at the destination, we will release another batch of this O-D pair. Repeat this process until finishing all batches of an O-D pair and continue another O-D pair.
- In each batch, only when all the AVs in this batch arrive at the downstream queue in each link, we will release them into the next link in the selected path. The time of passing link  $(i, j)$  for batch  $B^{r',s'}$  is denoted by  $T_{i,j}^{r',s'}$ .

Therefore, the total time consumed by above three steps is  $T_l + \sum_{(r',s')} n^{r',s'} \sum_{(i,j) \text{ in } P^{r',s'}} T_{i,j}^{r',s'}$ . If we choose the time horizon  $T$  that is larger than  $T_l + \sum_{(r',s')} n^{r',s'} \sum_{(i,j) \text{ in } P^{r',s'}} T_{i,j}^{r',s'}$ , we could construct a solution so that the problem is feasible. To this end, we present the details of how to construct the flow as follows.

In order to satisfy the queue capacity constraint in Equation 12, the size of batch should be constrained as follows:

$$B^{r',s'} < \min_{(i,j) \text{ in } P^{r',s'}} \{\bar{Q}_{i,j}^U, \bar{Q}_{i,j}^D\}.$$

After determining the size of each batch, the next step is to determine the flow rate of each batch. Suppose we release the batch at a constant rate, so  $B^{r',s'} = T_B^{r',s'} F_B^{r',s'}$ , where  $T_B^{r',s'}$  is the time of releasing all batches once and  $F_B^{r',s'}$  is the flow rate of releasing all batches once. In order to satisfy the inflow and outflow capacity constraints in Equation 13, we keep free-flow state rather than congested state in the flow area in each link and we desire the flow rate  $F_B^{r',s'}$  wouldn't be too small to make sure the density in this period is larger than  $\frac{1}{L_{i,j}}$ , the flow rate  $F_B^{r',s'}$  should be constrained as follows:

$$\max_{(i,j) \text{ in } P^{r',s'}} \left\{ \frac{v_{i,j}^f}{L_{i,j}} \right\} \leq F_B^{r',s'} < \min_{(i,j) \text{ in } P^{r',s'}} \left\{ \bar{C}_{i,j}^\mu, \bar{C}_{i,j}^v, \frac{v_{i,j}^f}{h_{i,j}^{\max}(t)v_{i,j}^f + L} \right\}.$$

Normally, the flow capacity is always larger than  $\frac{v_{i,j}^f}{L_{i,j}}$ . It is meaningless to discuss the maximin headway control under the case that the flow capacity is extremely small that we only allow a small number of vehicle to enter or exit the link. Otherwise, when releasing all AVs in this batch, the density in link  $(i, j)$  is already smaller than  $\frac{1}{L_{i,j}}$ , which already satisfies the end constraint. So in this case  $T_{i,j}^{r',s'} = T_B^{r',s'}$ .

Then we calculate  $T_{i,j}^{r',s'}$ , which represents the time of passing link  $(i, j)$  for batch  $B^{r',s'}$  and  $T_{i,j}^{r',s'}$  is comprised of three time periods:

- Only  $u_{i,j}(t)$  exists. This time period means that the first vehicle entering the link  $(i, j)$  will drive in a free-flow speed  $v_{i,j}^f$  and the time of this period is  $\tau_{i,j}^f = \frac{L_{i,j}}{v_{i,j}^f}$ . And the density of link  $(i, j)$  at time  $\tau_{i,j}^f$  is  $\rho_{i,j}(\tau_{i,j}^f) = \frac{F_B^{r',s'}}{L_{i,j}} \frac{L_{i,j}}{v_{i,j}^f} = \frac{F_B^{r',s'}}{v_{i,j}^f}$ .
- Both  $u_{i,j}(t)$  and  $v_{i,j}(t)$  exist. This time period means that we still release the batch from prior link in this batch to link  $(i, j)$  and also exists flow  $f_{i,j}(t)$  which represents the inflow at the boundary between the flow area and buffer area of link  $(i, j)$ . Besides,  $\dot{\rho}_{i,j}(\tau_{i,j}^f) = \frac{u_{i,j}(\tau_{i,j}^f) - f_{i,j}(\tau_{i,j}^f)}{L_{i,j}} = \frac{F_B^{r',s'} - v_{i,j}^f \frac{F_B^{r',s'}}{v_{i,j}^f}}{L_{i,j}} = 0$ . So when  $\tau_{i,j}^f \leq t \leq T_B^{r',s'}$ , we have  $u_{i,j}(t) = f_{i,j}(t) = F_B^{r',s'}$  and  $\rho_{i,j}(t) = \frac{F_B^{r',s'}}{L_{i,j}}$ .
- Only  $v_{i,j}(t)$  exists. This time period means that there is no releasing flow of batch from prior link and the end constraint is  $\rho_{i,j}(T) < \frac{1}{L_{i,j}}$ . So we solve the following equations and derive  $T_{i,j}^{r',s'} = T_B^{r',s'} + \frac{L_{i,j}}{v_{i,j}^f} \ln \frac{L_{i,j} F_B^{r',s'}}{v_{i,j}^f}$ .

$$\begin{cases} \dot{\rho}_{i,j}(t) = \frac{u_{i,j}(t) - f_{i,j}(t)}{L_{i,j}} = \frac{-v_{i,j}^f \rho_{i,j}(t)}{L_{i,j}} \\ \rho_{i,j}(T_B^{r',s'}) = \frac{F_B^{r',s'}}{L_{i,j}} \\ \rho_{i,j}(T_{i,j}^{r',s'}) = \frac{1}{L_{i,j}} \end{cases}$$

It is obvious that other constraints are satisfied by constructing the solution based on above procedures. Therefore, if we choose the time horizon  $T$  so that  $T$  is larger than  $T_l + \sum_{(r',s')} n^{r',s'} \sum_{(i,j)} T_{i,j}^{r',s'} \delta_{i,j}^{P^{r',s'}}$ , where  $\delta_{i,j}^{P^{r',s'}}$  indicates whether link  $(i, j)$  is in the path  $P^{r',s'}$ , then we could always find a feasible solution of proposed problem.

## Appendix E. Sensitivity analysis of the headway control for SO-DTA

This section proposes a sensitivity-based algorithm to solve the SO-DTA problem. We first transform the discretized version of the headway-dependent SO-DTA formulation into mixed integer linear programming (MILP) given an exogenous headway variable  $\mathbf{h}$ , as shown in [Appendix E.1](#), then the sensitivity-based algorithm is presented.

### Appendix E.1. MILP formulation

This section transforms the discretized version of SO-DTA problem formulation from [Equations 22 to 39](#) into MILP. Although we transform it as MILP, it is easy to be solved by CPLEX and the  $\delta^*$  in solution of MILP benefits the analysis of traffic dynamics and maximin headway. Besides, we are also able to transform the problem from [Equations 22 to 39](#) into linear programming (LP) if we regard the piecewise function in [Equations 23 and 24](#) as the minimum value of two strightlines.

The objective of [section 4](#) is to find the optimal headway  $\{h_{i,j}(k)\}$ . In the proposed programming, the involved variables include  $\{\rho_{i,j}(k)\}$ ,  $\{\rho_{i,j}^{s'}(k)\}$ ,  $\{q_{i,j}^D(k)\}$ ,  $\{q_{i,j}^{D,s'}(k)\}$ ,  $\{q_{i,j}^U(k)\}$ ,  $\{q_{i,j}^{U,s'}(k)\}$ ,  $\{u_{i,j}(k)\}$ ,  $\{u_{i,j}^{s'}(k)\}$ ,  $\{f_{i,j}(k)\}$ ,  $\{f_{i,j}^{s'}(k)\}$ ,  $\{v_{i,j}(k)\}$ ,  $\{v_{i,j}^{s'}(k)\}$ ,  $\{n_{i,j}(k)\}$ ,  $\{h_{i,j}(k)\}$  and  $\{\delta_{i,j}(k)\}$ , where binary variables  $\{\delta_{i,j}(k)\}$  is used to indicate whether the flow area of link  $(i, j)$  in the  $k$ th time interval is congested or not. However, the proposed problem is hard to solve due to the nonlinearity in [Equations 23 to 24 and 26 to 27](#).

We note that if the headway  $\{h_{i,j}(k)\}$  is fixed, then the variables are  $\{\rho_{i,j}(k)\}$ ,  $\{\rho_{i,j}^{s'}(k)\}$ ,  $\{q_{i,j}^D(k)\}$ ,  $\{q_{i,j}^{D,s'}(k)\}$ ,  $\{q_{i,j}^U(k)\}$ ,  $\{q_{i,j}^{U,s'}(k)\}$ ,  $\{u_{i,j}(k)\}$ ,  $\{u_{i,j}^{s'}(k)\}$ ,  $\{f_{i,j}(k)\}$ ,  $\{f_{i,j}^{s'}(k)\}$ ,  $\{v_{i,j}(k)\}$ ,  $\{v_{i,j}^{s'}(k)\}$ ,  $\{n_{i,j}(k)\}$  and  $\{\delta_{i,j}(k)\}$ . Hence the proposed formulation becomes a mixed integer linear programming program (MILP).

For simplicity in notations, we use a generalized form of mixed integer linear programming to represent the formulation, as shown in [Equation E.1](#).

$$\begin{aligned} \min_{\mathbf{x}} \quad & TTT = \mathbf{P}^T \mathbf{x} \\ \text{s.t.} \quad & \mathbf{A}(\mathbf{h})\mathbf{x} = \mathbf{B}(\mathbf{h}) \\ & \mathbf{C}(\mathbf{h})\mathbf{x} \leq \mathbf{D}(\mathbf{h}) \end{aligned} \quad (\text{E.1})$$

where we have:

- $\mathbf{x} = \{\rho_{i,j}(k), \rho_{i,j}^{s'}(k), q_{i,j}^D(k), q_{i,j}^{D,s'}(k), q_{i,j}^U(k), q_{i,j}^{U,s'}(k), u_{i,j}(k), u_{i,j}^{s'}(k), f_{i,j}(k), f_{i,j}^{s'}(k), v_{i,j}(k), v_{i,j}^{s'}(k), n_{i,j}(k), \delta_{i,j}(k)\}$  for  $(i,j) \in E$ ,  $1 \leq k \leq N$ ;  $s' \in \bar{S}$ , and the dimension of variables  $\mathbf{x}$  is  $n$ .

- $\mathbf{h} = \{h_{i,j}(k) \mid (i,j) \in E \setminus (L_R \cup L_S); 1 \leq k \leq N\} \in \mathfrak{X}^m$ , and the dimension of parameters  $\mathbf{h}$  is  $m$ .

- $\mathbf{A}(\mathbf{h}) = \begin{bmatrix} a_1(\mathbf{h}) \\ \vdots \\ a_{l_1}(\mathbf{h}) \end{bmatrix} = \begin{bmatrix} a_{11}(\mathbf{h}) & \cdots & a_{1n}(\mathbf{h}) \\ \vdots & \ddots & \vdots \\ a_{l_1 1}(\mathbf{h}) & \cdots & a_{l_1 n}(\mathbf{h}) \end{bmatrix} \in \mathfrak{X}^{l_1 \times n}$ ;  $\mathbf{B}(\mathbf{h}) = \begin{bmatrix} b_1(\mathbf{h}) \\ \vdots \\ b_{l_1}(\mathbf{h}) \end{bmatrix} \in \mathfrak{X}^{l_1}$ .  $l_1$  represents the number of equality constraints.

- $\mathbf{C}(\mathbf{h}) = \begin{bmatrix} c_1(\mathbf{h}) \\ \vdots \\ c_{l_2}(\mathbf{h}) \end{bmatrix} = \begin{bmatrix} c_{11}(\mathbf{h}) & \cdots & a_{1n}(\mathbf{h}) \\ \vdots & \ddots & \vdots \\ c_{l_2 1}(\mathbf{h}) & \cdots & c_{l_2 n}(\mathbf{h}) \end{bmatrix} \in \mathfrak{X}^{l_2 \times n}$ ;  $\mathbf{D}(\mathbf{h}) = \begin{bmatrix} d_1(\mathbf{h}) \\ \vdots \\ d_{l_2}(\mathbf{h}) \end{bmatrix} \in \mathfrak{X}^{l_2}$ .  $l_2$  represents the number of inequality constraints.

### Appendix E.2. Sensitivity-based optimal headway control solution algorithm

We then present the sensitivity analysis for the developed MILP, and the focus is to derive the gradient of TTT with respect to the headway. The Lagrange multiplier of [Equation E.1](#) is shown in [Equation E.2](#) and the corresponding Karush–Kuhn–Tucker (KKT) conditions are presented from [Equations E.3 to E.7](#).

$$\min_{\mathbf{x}} \quad L = \mathbf{P}^T \mathbf{x} + \lambda^T (\mathbf{A}(\mathbf{h})\mathbf{x} - \mathbf{B}(\mathbf{h})) + \mu^T (\mathbf{C}(\mathbf{h})\mathbf{x} - \mathbf{D}(\mathbf{h})) \quad (\text{E.2})$$

$$\mathbf{P}^T + \lambda^{*T} \mathbf{A}(\mathbf{h}) + \mu^{*T} \mathbf{C}(\mathbf{h}) = \mathbf{0} \quad (\text{E.3})$$

$$\mathbf{A}(\mathbf{h})\mathbf{x}^* = \mathbf{B}(\mathbf{h}) \quad (\text{E.4})$$

$$\mathbf{C}(\mathbf{h})\mathbf{x}^* \leq \mathbf{D}(\mathbf{h}) \quad (\text{E.5})$$

$$\mu_i^* (\mathbf{C}(\mathbf{h})\mathbf{x}^* - \mathbf{D}(\mathbf{h}))_i = \mathbf{0} \quad (\text{E.6})$$

$$\mu^* \geq \mathbf{0} \quad (\text{E.7})$$

where,

- $\lambda^* \in \mathfrak{X}^{l_1}$  and  $\mu^* \in \mathfrak{X}^{l_2}$ .
- $K = \{i \mid \mu_i^* > 0; 1 \leq i \leq l_2\}$  is the set of index of all positive  $\mu_i^*$ . And the size of  $K$  is  $k$ . If  $i \in K$ , then  $\mu_i^* > 0$ .

Then we do the differential to the Equation E.1 as  $\mathbf{z} = \mathbf{P}^T \mathbf{X}$  and Equations E.3 to E.6.

$$\mathbf{P}^T d\mathbf{x} - d\mathbf{z} = 0 \quad (\text{E.8})$$

$$\left( \sum_{i=1}^{l_1} \lambda_i^* \nabla_{\mathbf{h}} a_i(\mathbf{h}) + \sum_{j=1}^{l_2} \mu_j^* \nabla_{\mathbf{h}} c_j(\mathbf{h}) \right) d\mathbf{h} + (\mathbf{A}(\mathbf{h}))^T d\lambda + (\mathbf{C}(\mathbf{h}))^T d\mu = \mathbf{0} \quad (\text{E.9})$$

$$\mathbf{A}(\mathbf{h})d\mathbf{x} + [\nabla_{\mathbf{h}}(\mathbf{A}(\mathbf{h})\mathbf{x}^*) - \nabla_{\mathbf{h}}\mathbf{B}(\mathbf{h})] d\mathbf{h} = \mathbf{0} \quad (\text{E.10})$$

$$\mathbf{C}_k(\mathbf{h})d\mathbf{x} + [\nabla_{\mathbf{h}}(\mathbf{C}_k(\mathbf{h})\mathbf{x}^*) - \nabla_{\mathbf{h}}\mathbf{D}_k(\mathbf{h})] d\mathbf{h} = \mathbf{0} \quad (\text{E.11})$$

where,

$$\bullet \nabla_{\mathbf{h}} a_i(\mathbf{h}) = \nabla_{\mathbf{h}} \begin{bmatrix} a_{i1}(\mathbf{h}) & \cdots & a_{in}(\mathbf{h}) \end{bmatrix} = \begin{bmatrix} \frac{\partial a_{i1}(\mathbf{h})}{\partial \mathbf{h}_1} & \cdots & \frac{\partial a_{i1}(\mathbf{h})}{\partial \mathbf{h}_m} \\ \vdots & \ddots & \vdots \\ \frac{\partial a_{in}(\mathbf{h})}{\partial \mathbf{h}_1} & \cdots & \frac{\partial a_{in}(\mathbf{h})}{\partial \mathbf{h}_m} \end{bmatrix} \in \mathfrak{X}^{n \times m}$$

$$\bullet \nabla_{\mathbf{h}} c_j(\mathbf{h}) = \nabla_{\mathbf{h}} \begin{bmatrix} c_{j1}(\mathbf{h}) & \cdots & c_{jn}(\mathbf{h}) \end{bmatrix} = \begin{bmatrix} \frac{\partial c_{j1}(\mathbf{h})}{\partial \mathbf{h}_1} & \cdots & \frac{\partial c_{j1}(\mathbf{h})}{\partial \mathbf{h}_m} \\ \vdots & \ddots & \vdots \\ \frac{\partial c_{jn}(\mathbf{h})}{\partial \mathbf{h}_1} & \cdots & \frac{\partial c_{jn}(\mathbf{h})}{\partial \mathbf{h}_m} \end{bmatrix} \in \mathfrak{X}^{n \times m}$$

$$\bullet \mathbf{A}^x = \mathbf{A}(\mathbf{h})\mathbf{x}^* = \begin{bmatrix} a_1^x(x^*, \mathbf{h}) \\ \vdots \\ a_{l_1}^x(x^*, \mathbf{h}) \end{bmatrix} \in \mathfrak{X}^{l_1}; \nabla_{\mathbf{h}} \mathbf{A}^x = \begin{bmatrix} \frac{\partial a_1^x(x^*, \mathbf{h})}{\partial \mathbf{h}_1} & \cdots & \frac{\partial a_1^x(x^*, \mathbf{h})}{\partial \mathbf{h}_m} \\ \vdots & \ddots & \vdots \\ \frac{\partial a_{l_1}^x(x^*, \mathbf{h})}{\partial \mathbf{h}_1} & \cdots & \frac{\partial a_{l_1}^x(x^*, \mathbf{h})}{\partial \mathbf{h}_m} \end{bmatrix} \in \mathfrak{X}^{l_1 \times m}$$

$$\bullet \mathbf{C}_k(\mathbf{h}) = \begin{bmatrix} \vdots \\ c_j(\mathbf{h}) \\ \vdots \end{bmatrix}_{j \in K} \in \mathfrak{X}^{k \times n}; \mathbf{C}_k^x = \mathbf{C}_k(\mathbf{h})\mathbf{x}^* = \begin{bmatrix} \vdots \\ c_j^x(x^*, \mathbf{h}) \\ \vdots \end{bmatrix}_{j \in K} \in \mathfrak{X}^k; \mathbf{D}_k(\mathbf{h}) = \begin{bmatrix} \vdots \\ d_j(\mathbf{h}) \\ \vdots \end{bmatrix}_{j \in K} \in \mathfrak{X}^k$$

$$\bullet \nabla_{\mathbf{h}} \mathbf{C}_{\mathbf{k}}^x = \left[ \begin{array}{ccc} \vdots & \cdots & \vdots \\ \frac{\partial c_j^x(x^*, \mathbf{h})}{\partial \mathbf{h}_1} & \cdots & \frac{\partial c_j^x(x^*, \mathbf{h})}{\partial \mathbf{h}_m} \\ \vdots & \cdots & \vdots \end{array} \right]_{j \in K} \in \mathfrak{R}^{k \times m}$$

We cast Equations E.8 to E.11 into the form of block matrices.

$$\left[ \begin{array}{cccc} \mathbf{P}^T & \mathbf{0} & \mathbf{0} & -1 \\ \mathbf{0} & (\mathbf{A}(\mathbf{h}))^T & (\mathbf{C}(\mathbf{h}))^T & \mathbf{0} \\ \mathbf{A}(\mathbf{h}) & \mathbf{0} & \mathbf{0} & \mathbf{0} \\ \mathbf{C}_{\mathbf{k}}(\mathbf{h}) & \mathbf{0} & \mathbf{0} & \mathbf{0} \end{array} \right] \begin{bmatrix} d\mathbf{x} \\ d\lambda \\ d\mu \\ dz \end{bmatrix} = - \left[ \begin{array}{c} \mathbf{0} \\ \sum_{i=1}^{l_1} \lambda_i^* \nabla_{\mathbf{h}} a_i(\mathbf{h}) + \sum_{j=1}^{l_2} \mu_j^* \nabla_{\mathbf{h}} c_j(\mathbf{h}) \\ \nabla_{\mathbf{h}} (\mathbf{A}(\mathbf{h})\mathbf{x}^*) - \nabla_{\mathbf{h}} \mathbf{B}(\mathbf{h}) \\ \nabla_{\mathbf{h}} (\mathbf{C}_{\mathbf{k}}(\mathbf{h})\mathbf{x}^*) - \nabla_{\mathbf{h}} \mathbf{D}_{\mathbf{k}}(\mathbf{h}) \end{array} \right] d\mathbf{h} \quad (\text{E.12})$$

We further define

$$\mathbf{Q} = \left[ \begin{array}{cccc} \mathbf{P}^T & \mathbf{0} & \mathbf{0} & -1 \\ \mathbf{0} & (\mathbf{A}(\mathbf{h}))^T & (\mathbf{C}(\mathbf{h}))^T & \mathbf{0} \\ \mathbf{A}(\mathbf{h}) & \mathbf{0} & \mathbf{0} & \mathbf{0} \\ \mathbf{C}_{\mathbf{k}}(\mathbf{h}) & \mathbf{0} & \mathbf{0} & \mathbf{0} \end{array} \right]. \quad (\text{E.13})$$

The dimension of matrix  $\mathbf{Q}$  is  $(n + l_1 + k + 1) \times (n + l_1 + l_2 + 1)$ . If there exists  $\mu_i^* = 0$ , then the matrix  $\mathbf{Q}$  is not a square matrix and hence not invertible. So we calculate the generalized inverse matrix of  $\mathbf{Q}$  and denote it as  $\mathbf{Q}^{-1}$  (Penrose 1955).

$$\begin{bmatrix} d\mathbf{x} \\ d\lambda \\ d\mu \\ dz \end{bmatrix} = -\mathbf{Q}^{-1} \left[ \begin{array}{c} \mathbf{0} \\ \sum_{i=1}^{l_1} \lambda_i^* \nabla_{\mathbf{h}} a_i(\mathbf{h}) + \sum_{j=1}^{l_2} \mu_j^* \nabla_{\mathbf{h}} c_j(\mathbf{h}) \\ \nabla_{\mathbf{h}} (\mathbf{A}(\mathbf{h})\mathbf{x}^*) - \nabla_{\mathbf{h}} \mathbf{B}(\mathbf{h}) \\ \nabla_{\mathbf{h}} (\mathbf{C}_{\mathbf{k}}(\mathbf{h})\mathbf{x}^*) - \nabla_{\mathbf{h}} \mathbf{D}_{\mathbf{k}}(\mathbf{h}) \end{array} \right] d\mathbf{h} \quad (\text{E.14})$$

Then we replace  $d\mathbf{h}$  with the identity matrix  $I_m$  and derive the gradient  $\frac{\partial \mathbf{z}}{\partial \mathbf{h}}$ .

$$\begin{bmatrix} \frac{\partial \mathbf{x}}{\partial \mathbf{h}} \\ \frac{\partial \lambda}{\partial \mathbf{h}} \\ \frac{\partial \mu}{\partial \mathbf{h}} \\ \frac{\partial \mathbf{z}}{\partial \mathbf{h}} \end{bmatrix} = -\mathbf{Q}^{-1} \left[ \begin{array}{c} \mathbf{0} \\ \sum_{i=1}^{l_1} \lambda_i^* \nabla_{\mathbf{h}} a_i(\mathbf{h}) + \sum_{j=1}^{l_2} \mu_j^* \nabla_{\mathbf{h}} c_j(\mathbf{h}) \\ \nabla_{\mathbf{h}} (\mathbf{A}(\mathbf{h})\mathbf{x}^*) - \nabla_{\mathbf{h}} \mathbf{B}(\mathbf{h}) \\ \nabla_{\mathbf{h}} (\mathbf{C}_{\mathbf{k}}(\mathbf{h})\mathbf{x}^*) - \nabla_{\mathbf{h}} \mathbf{D}_{\mathbf{k}}(\mathbf{h}) \end{array} \right] \quad (\text{E.15})$$

Therefore, a sensitivity-based optimal headway control algorithm is proposed based on exploring the gradient descent of TTT, as shown in Algorithm 2.

---

#### Algorithm 2 Sensitivity-based Optimal Headway Solving Algorithm

---

**Input:** learning rate  $\eta$ .

**Output:** time-dependent and link-specific headway  $\{h_{i,j}(k)\}$ .

Initialize the headway  $\mathbf{h}$ .

- 1: **for** ( $i = 0; i < I; ++ i$ ) **do**
- 2:   Solve the Formulation E.1 given the current headway setting  $\mathbf{h}$  and derive  $\mathbf{z}^*, \lambda^*, \mu^*$  and  $\mathbf{x}^*$ .
- 3:   Conduct the sensitivity analysis and derive  $\frac{\partial \mathbf{z}^*}{\partial \mathbf{h}}$ .
- 4:   Update the headway by  $\mathbf{h} = \mathbf{h} - \eta \frac{\partial \mathbf{z}^*}{\partial \mathbf{h}}$ .
- 5: **end for**

**Return:** optimal headway  $\mathbf{h}^*$ .

---

#### Appendix F. Proof of Proposition 4

We first present Lemma 1 to show that a smaller headway  $h_{i,j}(k)$  could generate a larger flow  $f_{i,j}(k)$ .

**Lemma 1.** Given  $u_{i,j}(k)$  and  $\rho_{i,j}(k-1)$ , if  $h_{i,j}^{(1)}(k) \leq h_{i,j}^{(2)}(k)$ , then  $f_{i,j}^{(1)}(k) \geq f_{i,j}^{(2)}(k)$ .

*Proof.* We solve  $f_{i,j}(k)$  and  $\rho_{i,j}(k)$  under given  $u_{i,j}(k)$  and  $\rho_{i,j}(k-1)$  in both free-flow and congested states:

- Free-flow state:

$$\begin{cases} f_{i,j}(k) = v_{i,j}^f \rho_{i,j}(k) \\ \rho_{i,j}(k) = \rho_{i,j}(k-1) + \Delta_t \frac{u_{i,j}(k) - f_{i,j}(k)}{L_{i,j}} \end{cases}$$

Then we obtain the following equations:

$$\begin{cases} f_{i,j}(k) = \frac{L_{i,j} v_{i,j}^f \rho_{i,j}(k-1) + \Delta_t v_{i,j}^f u_{i,j}(k)}{L_{i,j} + \Delta_t v_{i,j}^f} \\ \rho_{i,j}(k) = \frac{L_{i,j} \rho_{i,j}(k-1) + \Delta_t u_{i,j}(k)}{L_{i,j} + \Delta_t v_{i,j}^f} \end{cases}$$

- Congested state:

$$\begin{cases} f_{i,j}(k) = \frac{1 - \rho_{i,j}(k)}{h_{i,j}(k)} L \\ \rho_{i,j}(k) = \rho_{i,j}(k-1) + \Delta_t \frac{u_{i,j}(k) - f_{i,j}(k)}{L_{i,j}} \end{cases}$$

Then the two quantities can be derived as:

$$\begin{cases} f_{i,j}(k) = \frac{L_{i,j} - L_{i,j} \rho_{i,j}(k-1) - L \Delta_t u_{i,j}(k)}{L_{i,j} h_{i,j}(k) - L \Delta_t} \\ \rho_{i,j}(k) = \frac{h_{i,j}(k) L_{i,j} \rho_{i,j}(k-1) + h_{i,j}(k) \Delta_t u_{i,j}(k) - \Delta_t}{L_{i,j} h_{i,j}(k) - L \Delta_t} \end{cases}$$

Next, We will discuss different states of  $\rho_{i,j}^{(2)}(k)$ :

- If  $\rho_{i,j}^{(2)}(k)$  is under free-flow state: Because  $h_{i,j}^{(1)}(k) \leq h_{i,j}^{(2)}(k)$ , as is shown in Figure 2, it is obvious that  $f_{i,j}^{(1)}(k) = f_{i,j}^{(2)}(k)$ .
- If  $\rho_{i,j}^{(2)}(k)$  is under congested state:

$$\begin{cases} \rho_{i,j}^{(2)}(k) = \frac{L_{i,j} \rho_{i,j}^{(2)}(k-1) + \Delta_t u_{i,j}^{(2)}(k)}{L_{i,j} + \Delta_t v_{i,j}^f} \geq \frac{1}{h_{i,j}^{(2)}(k) v_{i,j}^f + L} & \text{The density in free-flow state should be infeasible} \\ \rho_{i,j}^{(2)}(k) = \frac{h_{i,j}^{(2)}(k) L_{i,j} \rho_{i,j}^{(2)}(k-1) + h_{i,j}^{(2)}(k) \Delta_t u_{i,j}^{(2)}(k) - \Delta_t}{L_{i,j} h_{i,j}^{(2)}(k) - L \Delta_t} \geq \frac{1}{h_{i,j}^{(2)}(k) v_{i,j}^f + L} & \text{The density in congested state should be feasible} \end{cases}$$

For the free-flow state, if  $L_{i,j} h_{i,j}^{(2)}(k) - L \Delta_t < 0$ , we have

$$\begin{aligned} \rho_{i,j}^{(2)}(k) &= \frac{h_{i,j}^{(2)}(k) L_{i,j} \rho_{i,j}^{(2)}(k-1) + h_{i,j}^{(2)}(k) \Delta_t u_{i,j}^{(2)}(k) - \Delta_t}{L_{i,j} h_{i,j}^{(2)}(k) - L \Delta_t} \\ &\leq \frac{\frac{L_{i,j} + \Delta_t v_{i,j}^f}{h_{i,j}^{(2)}(k) v_{i,j}^f + L} h_{i,j}^{(2)}(k) - \Delta_t}{L_{i,j} h_{i,j}^{(2)}(k) - L \Delta_t} = \frac{1}{h_{i,j}^{(2)}(k) v_{i,j}^f + L} \end{aligned}$$

It is contradicted with  $\rho_{i,j}^{(2)}(k) \geq \frac{1}{h_{i,j}^{(2)}(k) v_{i,j}^f + L}$ . Therefore,  $L_{i,j} h_{i,j}^{(2)}(k) - L \Delta_t > 0$ . It is also similar to prove that if  $\rho_{i,j}(k)$  is congested under the headway  $h_{i,j}(k)$ , then  $L_{i,j} h_{i,j}(k) - L \Delta_t > 0$ .

Next, we discuss the states of  $\rho_{i,j}^{(1)}(k)$ .

\*  $\rho_{i,j}^{(1)}(k)$  is in congested state, then we have

$$\rho_{i,j}^{(1)}(k) = \frac{L_{i,j} \rho_{i,j}^{(2)}(k-1) + \Delta_t u_{i,j}^{(2)}(k)}{L_{i,j} + \Delta_t v_{i,j}^f} \geq \frac{1}{h_{i,j}^{(1)}(k) v_{i,j}^f + L} \geq \frac{1}{h_{i,j}^{(2)}(k) v_{i,j}^f + L}$$

The congested state of  $\rho_{i,j}^{(1)}(k)$  can be calculated as follows:

$$\begin{aligned} \rho_{i,j}^{(1)}(k) &= \frac{h_{i,j}^{(1)}(k) L_{i,j} \rho_{i,j}^{(2)}(k-1) + h_{i,j}^{(2)}(k) \Delta_t u_{i,j}^{(2)}(k) - \Delta_t}{L_{i,j} h_{i,j}^{(1)}(k) - L \Delta_t} \\ &\geq \frac{\frac{L_{i,j} + \Delta_t v_{i,j}^f}{h_{i,j}^{(1)}(k) v_{i,j}^f + L} h_{i,j}^{(1)}(k) - \Delta_t}{L_{i,j} h_{i,j}^{(1)}(k) - L \Delta_t} = \frac{1}{h_{i,j}^{(1)}(k) v_{i,j}^f + L} \end{aligned}$$

The flow  $f_{i,j}(k) = \frac{L_{i,j} - L L_{i,j} \rho_{i,j}^{(1)}(k-1) - L \Delta_t u_{i,j}(k)}{L_{i,j} h_{i,j}^{(1)}(k) - L \Delta_t}$  and we have proved that both numerator and denominator are positive, so if  $h_{i,j}^{(1)}(k) \leq h_{i,j}^{(2)}(k)$ , we have  $f_{i,j}^{(1)}(k) \geq f_{i,j}^{(2)}(k)$ .

\*  $\rho_{i,j}^{(1)}(k)$  is in free-flow state, then the free-flow state of  $\rho_{i,j}^{(1)}(k)$  should be feasible, as shown in the following equation.

$$\frac{1}{h_{i,j}^{(2)}(k) v_{i,j}^f + L} \leq \rho_{i,j}^{(1)}(k) = \frac{L_{i,j} \rho_{i,j}^{(2)}(k-1) + \Delta_t u_{i,j}^{(2)}(k)}{L_{i,j} + \Delta_t v_{i,j}^f} \leq \frac{1}{h_{i,j}^{(1)}(k) v_{i,j}^f + L}$$

Therefore, for the flow  $f_{i,j}^{(1)}(k)$ , we have:

$$f_{i,j}^{(1)}(k) = \frac{L_{i,j} v_{i,j}^f \rho_{i,j}^{(2)}(k-1) + \Delta_t v_{i,j}^f u_{i,j}^{(2)}(k)}{L_{i,j} + \Delta_t v_{i,j}^f} \geq \frac{v_{i,j}^f}{h_{i,j}^{(2)}(k) v_{i,j}^f + L} \geq f_{i,j}^{(2)}(k)$$

Combining the above proofs for the two states, we have  $f_{i,j}^{(1)}(k) \geq f_{i,j}^{(2)}(k)$  hold.  $\square$

Then we develop Lemma 2 to prove that the assumption of Lemma 1 is reachable, which means that when  $h_{i,j}^1(k) \leq h_{i,j}^2(k)$ , we could always find the feasible  $u_{i,j}(k)$  and  $\rho_{i,j}(k-1)$  for both  $h_{i,j}^1(k)$  and  $h_{i,j}^2(k)$ .

**Lemma 2.** For  $\mathbf{h}_1 = \{h_{i,j}^1(k)\}$  and  $\mathbf{h}_2 = \{h_{i,j}^2(k)\}$ , if there exist only one  $(i, j)$  and  $k$  such that  $h_{i,j}^1(k) \leq h_{i,j}^2(k)$  and  $h_{m,n}^1(l) = h_{m,n}^2(l)$  for other links  $(m, n) \neq (i, j)$  or time intervals  $l \neq k$ , suppose  $u_{i,j}^{s',(2)}(k) \in \mathbf{x}_2, \forall s'$ , where  $\mathbf{x}_2 \in \Omega_{\mathbf{h}_2}$ , then there always exists  $\mathbf{x}_1 \in \Omega_{\mathbf{h}_1}$ , such that  $u_{i,j}^{s',(1)}(k) \in \mathbf{x}_1$  and  $u_{i,j}^{s',(1)}(k) = u_{i,j}^{s',(2)}(k)$ .

*Proof.* In addition to the flow  $f_{i,j}(k)$ , headway affects the shockwave travel time  $n_{i,j}^w(k)$  as follows:

$$\begin{aligned} n_{i,j}^w(k) \Delta_t \frac{L}{h_{i,j}(k)} &\leq L_{i,j}, \\ (n_{i,j}^w(k) + 1) \Delta_t \frac{L}{h_{i,j}(k)} &> L_{i,j}. \end{aligned}$$

To show the existence of a feasible  $\mathbf{x}_1$  such that  $u_{i,j}^{s',(1)}(k) = u_{i,j}^{s',(2)}(k)$ , we need to show that  $u_{i,j}^{s',(2)}(k)$  satisfies the upstream queue capacity under  $h_{i,j}^1(k)$  and other related variables in  $\mathbf{x}_2$  if we set  $u_{i,j}^{s',(1)}(l) = u_{i,j}^{s',(2)}(l), \forall 1 \leq l \leq k-1$ . Therefore, we could also derive  $f_{i,j}^{s',(1)}(l) = f_{i,j}^{s',(2)}(l), \forall 1 \leq l \leq k-1$  by both the proof of Lemma 1 and the assumption that  $h_{i,j}^1(l) = h_{i,j}^2(l), \forall 1 \leq l \leq k-1$ .

If  $h_{i,j}^{(1)}(k) \leq h_{i,j}^{(2)}(k)$ , then  $n_{i,j}^{w,(1)}(k) \leq n_{i,j}^{w,(2)}(k)$ , which implies that if we use a smaller the headway in link  $(i, j)$  at the  $k_{th}$  time interval, the shockwave travel time would be smaller. By Equation 29, we have  $q_{i,j}^{u,s',(1)}(k) \leq q_{i,j}^{u,s',(2)}(k)$ . In order to keep  $u_{i,j}^{s',(2)}(k)$  unchanged under  $h_{i,j}^{(1)}(k)$ , we next prove  $q_{i,j}^{u,s',(1)}(k) \geq 0$ .

$$\begin{aligned}
q_{i,j}^{u,s',(1)}(k) &= \sum_{l=0}^k \Delta_t u_{i,j}^{s',(1)}(l) - \sum_{l=0}^{k-n_{i,j}^{w,(1)}(k)} \Delta_t f_{i,j}^{s',(1)}(l) \\
&= \sum_{l=0}^k \Delta_t u_{i,j}^{s',(2)}(l) - \sum_{l=0}^{k-n_{i,j}^{w,(1)}(k)} \Delta_t f_{i,j}^{s',(1)}(l) \\
&\geq \sum_{l=0}^k \Delta_t u_{i,j}^{s',(2)}(l) - \sum_{l=0}^{k-1} \Delta_t f_{i,j}^{s',(1)}(l) \\
&= \sum_{l=0}^k \Delta_t u_{i,j}^{s',(2)}(l) - \sum_{l=0}^{k-1} \Delta_t f_{i,j}^{s',(2)}(l) \\
&= L_{i,j} \rho_{i,j}^{s',(2)}(k-1) + \Delta_t u_{i,j}^{s',(2)}(k) \geq 0
\end{aligned}$$

□

By Lemma 1 and 2, for link  $(j, s)$ , where  $s \in S$ , if  $h_{j,s}^{(1)}(k) \leq h_{j,s}^{(2)}(k)$ ,  $h_{j,s}^{(1)}(l) = h_{j,s}^{(2)}(l)$ ,  $\forall l \neq k$  and we set  $u_{j,s}^{(1)}(l) = u_{j,s}^{(2)}(l)$  for all  $1 \leq l \leq N$ , we have  $f_{j,s}^{(1)}(k) \geq f_{j,s}^{(2)}(k)$ . For density, we have the following equation hold:

$$\rho_{j,s}(k) = \rho_{j,s}(k-1) + \Delta_t \frac{u_{j,s}(k) - f_{j,s}(k)}{L_{j,s}}. \quad (\text{F.1})$$

If  $\rho_{j,s}^{(1)}(k-1) = \rho_{j,s}^{(2)}(k-1)$ , then we have  $\rho_{i,j}^{(1)}(k) \leq \rho_{i,j}^{(2)}(k)$ . If  $\rho_{i,j}^{(2)}(k+1)$  is in the free-flow state, the following equations hold in the proof of Lemma 1 for  $\rho_{j,s}^{(2)}(k+1)$  and  $f_{j,s}^{(2)}(k+1)$ :

$$\begin{cases} f_{j,s}(k) = \frac{L_{j,s} v_{j,s}^f \rho_{j,s}(k-1) + \Delta_t v_{j,s}^f u_{j,s}(k)}{L_{j,s} + \Delta_t v_{j,s}^f} \\ \rho_{j,s}(k) = \frac{L_{i,j} \rho_{j,s}(k-1) + \Delta_t u_{j,s}(k)}{L_{j,s} + \Delta_t v_{j,s}^f} \end{cases}$$

So we have  $f_{i,j}^{(1)}(k+1) \leq f_{i,j}^{(2)}(k+1)$  and  $\rho_{i,j}^{(1)}(k+1) \leq \rho_{i,j}^{(2)}(k+1)$  if  $\rho_{i,j}^{(2)}(k+1)$  hold in the free-flow state. Then if  $\rho_{i,j}^{(2)}(k+1)$  is in the congested state, we have the following equations in the proof of Lemma 1 hold for  $\rho_{j,s}^{(2)}(k+1)$  and  $f_{j,s}^{(2)}(k+1)$ :

$$\begin{cases} f_{j,s}(k) = \frac{L_{j,s} - L_{j,s} \rho_{j,s}(k-1) - L_{j,s} \Delta_t u_{j,s}(k)}{L_{j,s} h_{j,s}(k) - L_{j,s} \Delta_t} \\ \rho_{j,s}(k) = \frac{h_{j,s}(k) L_{j,s} \rho_{j,s}(k-1) + h_{j,s}(k) \Delta_t u_{j,s}(k) - \Delta_t}{L_{j,s} h_{j,s}(k) - L_{j,s} \Delta_t} \end{cases}$$

Similarly,  $f_{i,j}^{(1)}(k+1) \geq f_{i,j}^{(2)}(k+1)$  and  $\rho_{i,j}^{(1)}(k+1) \leq \rho_{i,j}^{(2)}(k+1)$  hold for  $\rho_{i,j}^{(2)}(k+1)$  in the congested state.

Therefore, we have  $\rho_{i,j}^{(1)}(k+1) \leq \rho_{i,j}^{(2)}(k+1)$ . We conduct the same procedure for  $k+2, \dots, N$  and  $\rho_{i,j}^{(1)}(l) \leq \rho_{i,j}^{(2)}(l)$  is derived for  $l \geq k$  and  $\rho_{i,j}^{(1)}(l) = \rho_{i,j}^{(2)}(l)$  for  $l < k$ . Besides, by  $F_{j,s}(k) = L_{j,s} \rho_{j,s}(k) + U_{j,s}(k)$ , so we have  $F_{j,s}^{(1)}(l) = F_{j,s}^{(2)}(l)$  for  $l < k$  and  $F_{j,s}^{(1)}(l) \geq F_{j,s}^{(2)}(l)$  for  $l \geq k$ .

Similarly, we could also get the  $\rho_{j,s}^{s_0,(1)}(l) \leq \rho_{j,s}^{s_0,(2)}(l)$  for  $l \geq k$  and  $\rho_{i,j}^{s_0,(1)}(l) = \rho_{i,j}^{s_0,(2)}(l)$  for  $l < k$  by the same procedure for any destination  $s_0$ . Besides, for any destination  $s_0$ , we also have  $F_{j,s}^{s_0,(1)}(k) = F_{j,s}^{s_0,(2)}(k)$  for  $l < k$  and  $F_{j,s}^{s_0,(1)}(k) \geq F_{j,s}^{s_0,(2)}(k)$  for  $l \geq k$ .

Therefore, for destination  $s_0 \neq s$ , we could set  $v_{j,s}^{s_0,(1)}(l) = v_{j,s}^{s_0,(2)}(l)$ ,  $\forall 1 \leq l \leq N$ . For destination  $s$ , we have  $V_{j,s}^{s',(1)}(k) = V_{j,s}^{s',(2)}(k)$  for  $l < k$  and  $V_{j,s}^{s',(1)}(k) \geq V_{j,s}^{s',(2)}(k)$  for  $l \geq k$ , where  $V_{j,s}^{s'}(k) = \sum_{l=1}^k \Delta_t v_{j,s}^{s'}(l)$  represents the



cumulative outflow with destination  $s'$  of link  $(j, s)$  in the  $k$ th time interval. Then the total travel time in link  $(j, s)$  can be written as follows:

$$\begin{aligned}
TTT_{j,s} &= \sum_{k=1}^N \Delta_t \sum_{l=1}^k \Delta_t u_{j,s}(l) - v_{j,s}(l) \\
&= \sum_{k=1}^N \sum_{s_0} \Delta_t \Delta_t k u_{j,s}^{s_0}(k) - \Delta_t \Delta_t k v_{j,s}^{s_0}(k) \\
&= \sum_{k=1}^N \sum_{s_0 \neq s} \left( \Delta_t \Delta_t k u_{j,s}^{s_0}(k) - \Delta_t \Delta_t k v_{j,s}^{s_0}(k) \right) + \sum_{k=1}^N \left( \Delta_t \Delta_t k u_{j,s}^{s'}(k) - \Delta_t \Delta_t k v_{j,s}^{s'}(k) \right) \\
&= \sum_{k=1}^N \sum_{s_0 \neq s} \left( \Delta_t \Delta_t k u_{j,s}^{s_0}(k) - \Delta_t \Delta_t k v_{j,s}^{s_0}(k) \right) + \sum_{k=1}^N \Delta_t \Delta_t k u_{j,s}^{s'}(k) - \sum_{k=1}^N \Delta_t V_{j,s}^{s'}(k)
\end{aligned}$$

Therefore, we have proved that  $u_{j,s}^{s_0,(1)}(l) = u_{j,s}^{s_0,(2)}(l)$ ,  $v_{j,s}^{s_0,(1)}(l) = v_{j,s}^{s_0,(2)}(l)$  for  $s_0 \neq s$  and  $1 \leq l \leq N$ . For destination  $s$ , we have  $u_{j,s}^{s',(1)}(l) = u_{j,s}^{s',(2)}(k)$  and  $V_{j,s}^{s',(1)}(l) \geq V_{j,s}^{s',(2)}(l)$  for  $1 \leq l \leq N$ . Then we have

$$TTT_{j,s}^{(1)} \leq TTT_{j,s}^{(2)}.$$

The total travel time consists of the total travel time in link  $(j, s)$ , total travel time in other links and waiting time at origins. The inflow and outflow variables in other links and origins are not affected by the change of headway from  $h_{i,j}^{(1)}(k)$  to  $h_{i,j}^{(2)}(k)$ , so  $TTT_{h_1} \leq TTT_{h_2}$  if  $h_{i,j}^{(1)}(k) \leq h_{i,j}^{(2)}(k)$ . For link  $(i, j)$ , the node  $j$  acts like the destination node, and we want to push more flow with destination  $s$  to leave link  $(i, j)$  and enter link  $(j, s)$ . The process is similar to what we have done for link  $(j, s)$  by only changing one headway in link  $(i, j)$  and keep flow variables in other links unchanged. By repeating the above procedure for all the links and time intervals, we can show that TTT could be minimized under the minimum headway.

## Appendix G. Proof of Proposition 5

Suppose  $\mathbf{x}^*$  and  $\mathbf{h}^*$  are the optimal solution of the proposed SO-DTA problem. If  $\exists (i, j) \in E \setminus (L_R \cup L_S)$  and  $1 \leq k \leq N$ , s.t.  $\delta_{i,j}^*(k) = 0$ , we have following equations.

$$\begin{aligned}
0 &\leq \rho_{i,j}^*(k) < \frac{1}{h_{i,j}^*(k)v_{i,j}^f + L} \\
n_{i,j}^w(k) \Delta_t \frac{L}{h_{i,j}(k)} &\leq L_{i,j} \\
(n_{i,j}^w(k) + 1) \Delta_t \frac{L}{h_{i,j}(k)} &> L_{i,j}
\end{aligned}$$

For the following linear Equations G.1 to G.4 of  $h_{i,j}(k)$ , it is obvious that  $h_{i,j}^*(k)$  satisfies all of these equations.

$$\rho_{i,j}^*(k)v_{i,j}^f h_{i,j}(k) < 1 - \rho_{i,j}^*(k)L \quad (\text{G.1})$$

$$h_{i,j}(k) \geq \frac{\Delta_t L n_{i,j}^{w,*}(k)}{L_{i,j}} \quad (\text{G.2})$$

$$h_{i,j}(k) < \frac{\Delta_t L (n_{i,j}^{w,*}(k) + 1)}{L_{i,j}} \quad (\text{G.3})$$

$$h_{i,j}^{\min} \leq h_{i,j}(k) \leq h_{i,j}^{\max} \quad (\text{G.4})$$

If  $h_{i,j}^{\min} \leq h_{i,j}^*(k) < h_{i,j}^{\max}$ , Equations G.1 to G.4 could be formulated as following Equations G.5 and G.6 in general.

$$a_m x \geq b_m, \quad a_m > 0; b_m > 0; m = 1, \dots, M. \quad (\text{G.5})$$

$$c_n x < d_n, \quad c_n \geq 0; d_n \geq 0; n = 1, \dots, N. \quad (\text{G.6})$$

If there exists  $x$  satisfying Equations G.5 and G.6, then for any constant  $c$  with  $0 < c < \min\{\frac{b_m}{a_m}, 1\}$ , we have  $cx$  also satisfy Equations G.5 and G.6. Therefore, in this problem, there must exist such positive constant  $c$  that  $h_{i,j}(k) = ch_{i,j}^*(k)$  satisfies Equations G.1 to G.4. If  $h_{i,j}^*(k) = h_{i,j}^{max}$ , by Proposition 4, minimum headway setting achieves SO-DTA, so we show that SO-DTA can have at least two optimal headway that achieves the same TTT.

## Appendix H. Proof of Proposition 6

In Proposition 6, if  $\mathbf{x}^*$  with  $TTT(\mathbf{x}^*) = TTT^*$  is unique, then for  $\delta_{i,j}^*(k) = 1$ ,  $h_{i,j}^*(k)$  should satisfy the following equation.

$$f_{i,j}^*(k) = \frac{1 - \rho_{i,j}^*(k)L}{h_{i,j}^*(k)}$$

Therefore, if  $\hat{\mathbf{h}}$  and  $\bar{\mathbf{h}}$  are the solution of Formulation 40, we have  $\hat{h}_{i,j}(k) = \bar{h}_{i,j}(k)$  when  $\delta_{i,j}^*(k) = 1$ . Suppose  $\hat{\mathbf{h}} \neq \bar{\mathbf{h}}$ , then there must exist  $(i_1, j_1), (i_2, j_2) \in E$  and  $1 \leq k_1, k_2 \leq N$  such that  $\hat{h}_{i_1, j_1}(k_1) < \bar{h}_{i_1, j_1}(k_1)$  and  $\hat{h}_{i_2, j_2}(k_2) > \bar{h}_{i_2, j_2}(k_2)$ . Besides, we have  $\delta_{i_1, j_1}^*(k_1) = 0$  and  $\delta_{i_2, j_2}^*(k_2) = 0$ . So  $\hat{h}_{i_1, j_1}(k_1)$ ,  $\bar{h}_{i_1, j_1}(k_1)$ ,  $\hat{h}_{i_2, j_2}(k_2)$  and  $\bar{h}_{i_2, j_2}(k_2)$  should satisfy the Equations G.1 to G.4.

Therefore, if we construct a new headway  $\mathbf{h}$  as follows:

$$h_{i,j}(k) = \begin{cases} \hat{h}_{i,j}(k), & (i, j) \neq (i_1, j_1) \text{ or } k \neq k_1 \\ \bar{h}_{i,j}(k), & (i, j) = (i_1, j_1) \text{ and } k = k_1 \end{cases} \quad (\text{H.1})$$

We note that  $\mathbf{h}$  is the optimal headway of the discretized SO-DTA formulation (Equations 22 to 38) as  $\mathbf{x}^* \in \Omega_{\mathbf{h}}$ . However, we also have  $\|\mathbf{h}\|_1 > \|\hat{\mathbf{h}}\|_1$ , and this contradicts to the assumption that  $\hat{\mathbf{h}}$  is the solution of Formulation 40, which completes the proof.

## Appendix I. Proof of Proposition 7

Suppose  $\mathbf{x}^* \in \Omega_{\mathbf{h}^*}$  and  $TTT(\mathbf{x}^*) = TTT_{\mathbf{h}^*} = TTT^*$ , if  $\mathbf{h}$  satisfies Equation I.1:

$$\begin{aligned} \text{if } \delta_{i,j}^*(k) = 0 : \\ & \rho_{i,j}^*(k) v_{i,j}^f h_{i,j}(k) < 1 - \rho_{i,j}^*(k)L \\ & L_{i,j} h_{i,j}(k) \geq \Delta_t L n_{i,j}^{w,*}(k) \\ & L_{i,j} h_{i,j}(k) < \Delta_t L n_{i,j}^{w,*}(k) + \Delta_t L, \\ & h_{i,j}^*(k) < h_{i,j}(k) \leq h_{i,j}^{max} \end{aligned} \quad (\text{I.1})$$

$$\begin{aligned} \text{if } \delta_{i,j}^*(k) = 1 : \\ & h_{i,j}(k) = h_{i,j}^*(k) \end{aligned}$$

we have  $\|\mathbf{h}\|_1 > \|\mathbf{h}^*\|_1$  holds. Besides, it is obvious that  $\mathbf{x}^*$  and  $\mathbf{h}$  satisfy the Equations 23 and 39, so we have  $\mathbf{x}^* \in \Omega_{\mathbf{h}}$  and  $TTT_{\mathbf{h}} = TTT(\mathbf{x}^*) = TTT^*$ , which implies that  $\mathbf{h}$  is the optimal headway for SO-DTA. Therefore, we can construct such a larger optimal headway  $\mathbf{h}$  compared with the original optimal headway  $\mathbf{h}^*$ .

## Appendix J. Settings of the small network

For simplicity, the inflow capacity is set equal to the outflow capacity and the downstream queue capacity is set equal to the upstream queue capacity in each link. The detailed configurations of each link are presented in Table J.5.

Link	Flow capacity (vehicles/min)	Queue capacity (vehicles)	Free flow speed (km/min)	Link length (km)
1 → 3	50	600	1.2	3.6
1 → 4	45	600	1.1	3.3
2 → 3	45	600	1.2	3.6
2 → 4	50	600	1.1	3.3
3 → 5	60	600	1.0	4.0
4 → 5	60	600	1.0	3.0

Table J.5: Parameters settings in the small network.